INVESTIGATION OF ^{37}Cl
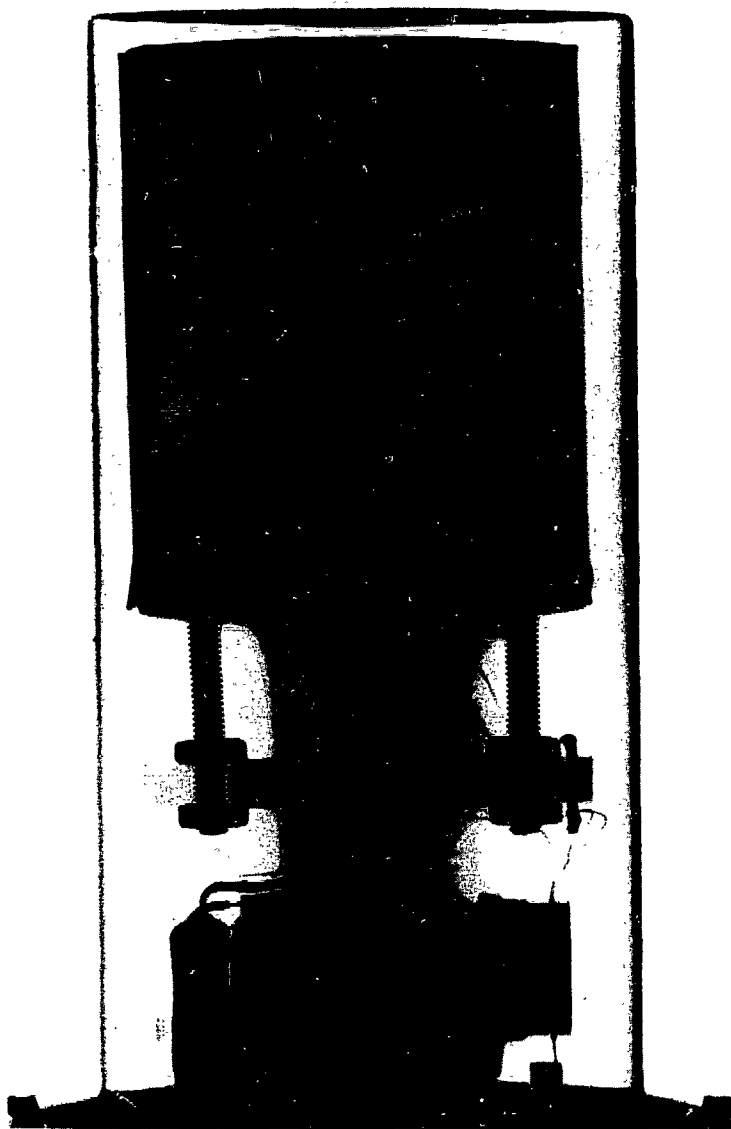# VIA
PROTON CAPTURE IN ^{36}S

G.J.L. NOOREN

Stellingen behorende bij het proefschrift

Investigation of ^{37}Cl via proton capture in ^{36}S

1. De spintoekenning J = 1/2 aan de ^{34}S(p,γ)^{35}Cl resonantie bij
   E_p= 832 keV door Meyer et al.[1] is juist, hoewel de gegeven
   argumentatie onvoldoende is [2].

   1) M.A. Meyer, I. Venter, W.F. Coetzee and D. Reitmann,
      Nucl.Phys. A246 (1976) 13
   2) Appendix A van dit proefschrift

2. De precisie waarmee hoge gamma-energieën uit vangstreacties
   worden bepaald, is vaak overschat, omdat
   a) niet-consistente ijkstandaarden zijn gebruikt,
   b) de door Helmer et al.[1] genoemde effecten niet in rekening
      zijn gebracht, en/of
   c) de detectiehoek onvoldoende nauwkeurig is bepaald.
   Gezien de grootte van deze effecten dienen alle bepalingen van
   Q-waarden in (p,γ), (α,γ) en (n,γ) reacties met een opgegeven
   nauwkeurigheid van beter dan 0,5 keV kritisch bekeken te worden.

   1) R.G. Helmer, J.E. Cline and R.C. Greenwood in The Electro-
      magnetic Interaction in Nuclear Spectroscopy, ed. W.D. Ha-
      milton (North-Holland, Amsterdam, 1975) p. 805

3. De gewoonte om gammastraling te karakteriseren met de foton-
   energie in plaats van met de golflengte heeft nadelige invloed
   op de nauwkeurigheid van de ijkstandaarden.

4. Indien men de dispersie van gammaspectra bepaalt met behulp van de afstanden tussen "foto"-piek en ontsnappingspieken, gaat men er ten onrechte van uit, dat de rustmassa van het elektron bepaald zou kunnen worden met een Ge-detector.

5. Bij het nauwkeurig meten van kleine proton-energieverschillen verdient modulatie van de proton-energie met een hoogspannings-voeding [1] de voorkeur boven modulatie van de stroom door de analysemagneet [2].

   1) *W. Duinker and C.R. Boersma, Observation of energyshifts due to K-shell ionisation in the reactions* $^{26}Mg(p,\gamma)^{27}Al$ *and* $^{27}Al(p,\gamma)^{28}Si$ *(wordt gepubliceerd)*
   2) *J.-F. Chemin, dissertatie, Bordeaux (1978)*

6. In publicaties over metingen van de deeltjesgrootte-verdelingen van aerosolen wordt veelal geen melding gemaakt van het detectierendement van de meetopstelling. Ten onrechte wordt hiermee de indruk gewekt, dat dit rendement geen belangrijke rol speelt.

7. Voor de bepaling van eigenschappen van atmosferische aerosolen is een tweekleuren laser-radar (LIDAR) te prefereren boven een eenkleurs LIDAR, vooral wanneer de gebruikte golflengtes ver uiteen liggen.

8. Door een analysemagneet wordt bundelenergiespreiding omgezet in bundelrichtingspreiding. Tenzij zeer nauwe spleten gebruikt worden, resulteert dit in een grotere onzekerheid van de bundelpositie in het vlak van afbuiging dan in het vlak loodrecht daarop. Het ver-dient daarom aanbeveling, draaitafel en analysemagneet niet in hetzelfde vlak te plaatsen.

9. Afbeeldingen van spectra waarbij langs de energie-as slechts kanaal-
   nummers zijn uitgezet, werken weinig verhelderend.

   Zie o.a.:
   G.I. Harris and J.J. Perrizo, Phys.Rev. C 2 (1970) 1347
   P.J. Nolan et al., J. of Phys. G 2 (1976) 569
   W. Biesiot, dissertatie, Groningen (1980)

10. De term "remote sensing" kan bijna altijd vervangen worden door
    het Nederlandse "aardobservatie".

11. Een op politici en bestuurders gerichte uiteenzetting van enige
    grondbeginselen van de thermodynamica zou bevorderlijk zijn voor
    de discussie over de energieproblematiek.

12. De emancipatie van de vrouw wordt bemoeilijkt door het feit dat
    voor veel vrouwen de keuze tussen maatschappelijke zekerheid en
    ontplooiing van de eigen talenten uitvalt ten voordele van het
    eerstgenoemde.

4 december 1980   G.J.L. Nooren

INVESTIGATION OF ^{37}Cl
VIA
PROTON CAPTURE IN ^{36}S

PROEFSCHRIFT

DOOR

GERARDUS JOHANNES LAMBERTUS NOOREN

GEBOREN OP 17 APRIL 1949 TE 'S-GRAVENHAGE

PROMOTOR: PROF. DR. C. VAN DER LEUN

Voorwoord

De voltooiing van dit proefschrift stelt mij in de gelegenheid om allen die aan de totstandkoming ervan hebben bijgedragen, te bedanken.

Allereerst dank ik mijn ouders, die mij als vanzelfsprekend altijd hebben aangespoord te "leren". Dit leerproces heeft nu geleid tot dit proefschrift.

Vervolgens gaat mijn erkentelijkheid uit naar mijn promotor, prof. C. van der Leun, voor zijn belangstelling en begeleiding. Beste Cor, je kritische opmerkingen hebben zowel de inhoud als de vorm van dit proefschrift op een aanzienlijk hoger peil gebracht. Dankzij je onverstoorbare inzet is dit werk op tijd gereedgekomen. De betekenis van de term "exponentiële begeleiding" is mij de laatste maanden exponentieel duidelijk geworden. Prof. P.M. Endt is als een stille kracht bij mijn onderzoek aanwezig geweest. Als bewaker van de "Utrechtse standaard" op spectroskopisch gebied, heeft hij zeker bijgedragen tot de kwaliteit van het werk.

De hulp van mijn collega's bij de 3 MV, R.J. Elsenaar, C. Alderliesten en E.L. Bakkum is onmisbaar geweest voor mijn onderzoek. Cees, Robert Jan en Eric, bedankt voor de fysica en de computers.

De technici van de 3 MV, Aart Veenenbos en Flip van der Vliet, hebben deze machine niet alleen uitstekend onderhouden, maar ook voortdurend verbeterd. Zonder hun inzet en kunde zouden experimenten op dit nivo niet mogelijk zijn geweest.

Adri Michielsen wil ik bedanken voor het vervaardigen van de trefplaatjes die zo'n belangrijke rol spelen bij dit werk. Met veel woorden maar altijd op tijd, werden de vreemdste trefplaatjes gemaakt.

De technische steun van Nico van Zwol, Tony van den Brink, Jan Sodaar en Dirk Balke werd zeer op prijs gesteld.

CONTENTS

CHAPTER 1

THE REACTION ^{36}S(p,γ)^{37}Cl

(I) Excitation energies and γ-ray branchings of bound states

deduced from resonances in the range E_p = 500 - 2000 keV

Abstract: Yield curves of the reaction ^{36}S(p,γ)^{37}Cl have been measured

over the range E_p = 500 - 2000 keV with a highly enriched (81 %)

^{36}S target. Proton energies, with a precision of typically 0.3 keV,

and strengths are presented for the nearly 200 observed resonances.

Several previously reported resonances, among which the well-known

J^π = 7/2$^-$, E_p = 1887 keV analogue resonance, are proven to be multi-

plets.

At 75 selected resonances in the ranges E_p = 500 - 1200 and

1800 - 2000 keV the decay schemes have been studied. These measure-

ments also provide rather detailed information on the γ-ray branching

ratios of more than 50 bound states of which the majority has not

been observed previously. Precision excitation energies have been

determined; for the levels with E_x < 5 MeV the median uncertainty

amounts to 30 ppm. The reaction Q-value is Q = 8386.34 ± 0.23 keV.

These precision data shed doubt on several previous spin and

parity assignments to low-lying bound states of ^{37}Cl. They also pro-

vide a basis for the lifetime measurements and spin and parity

assignments to be discussed in chapter II.

1. Introduction

Due to the low natural abundance of ^{36}S (0.017 %), the reaction ^{36}S(p,γ)^{37}Cl has so far not been studied very thoroughly. Apart from some very early experiments with NaI detectors, only two investigations with Ge(Li) detectors have been published. Hyder et al.[1] studied the range of proton energies of E_p = 800 - 1800 keV, using ^{36}S enriched to 3.5 %. Due to this low enrichment and the small size of their detectors, only strong resonances could be studied. Piiparinen et al.[2] used ^{36}S targets implanted with an isotope separator for the E_p = 1000 - 1900 keV range. Both groups measured decay schemes and lifetimes for a number of bound states of ^{37}Cl. The strong J^π = 7/2$^-$ analogue resonance at E_p = 1887 keV has been the subject of a more detailed study by both groups [3,4]. Because of the high resonance density and the rather poor energy resolution of the accelerators used in these measurements, it is likely that many resonances may have escaped detection.

The properties of the states of ^{37}Cl up to an excitation energy of $E_x \simeq$ 4 MeV are known in some detail [5]. In addition many states of ^{37}Cl are known at higher excitation energies, but the properties of most of these have not yet been determined. It should be mentioned, however, that this information is primarily due to studies of the ^{34}S(α,pγ)^{37}Cl reaction and only to a limited extent to the proton capture work quoted above.

When highly enriched (81 %) target material became available, it seemed worthwhile to use the good energy resolution of the Utrecht 3 MV Van de Graaff accelerator for a new study of the ^{36}S(p,γ)^{37}Cl reaction. Special attention has been given to the hitherto unexplored

regions, viz. E_p < 800 keV and E_p > 1900 keV up to the (p,n) threshold.

In proton capture reactions it is possible to excite low-spin states with relatively high excitation energies at low incident particle energies. From the many resonances, one can choose those which decay selectively to the levels of interest. In other reactions the selection of a particular bound state is usually accomplished by coincidence techniques. This necessity offsets to a large extent the larger cross sections of those reactions. This relative advantage holds of course only for low-spin states, since (p,γ) resonances with l > 4 are usually very weak at the energies that are most profitable for the study of resonance reactions.

2. Apparatus

In the measurements described here, the proton beam was obtained from the Utrecht 3 MV Van de Graaff accelerator. This machine is equipped with a 90° deflection magnet and a feedback corona stabilization system, that makes it possible to obtain beam energy spreads of 120 eV at E_p = 1 MeV [6].

The targets used consist of Ag_2S and were made following the prescriptions of Sterrenburg et al.[7]. A suspension in ethanol of elemental sulphur, enriched to 81 % in ^{36}S *), is dripped on a silver layer evaporated onto a tantalum backing, which is heated to about 100 ^{O}C. After evaporation of the ethanol the sulphur reacts with the silver to form Ag_2S. A sufficient number of drops is applied to ensure complete

---

*) Obtained from V/O Techsnabexport, Moscow.

saturation of the silver layer with sulphur. The target thickness then depends almost entirely on the thickness of the silver layer. Targets as thin as ≈ 0.5 keV at E_p = 2 MeV have been prepared with 4 $\mu g/cm^2$ silver. The very troublesome background caused by the ^{19}F + p and ^{23}Na + p reactions was reduced by heating the Ta backing [†] to incandescence under vacuum for several minutes, prior to evaporating the silver. Carbon contamination was kept low by taking special precautions during the preparation of the sulphur suspension. Glass vessels and pure ("spec-pure") ethanol were used exclusively. The suspension was never brought into contact with plastic or rubber. To minimize carbon deposition during the measurement, a liquid nitrogen cooled trap was placed in front of the target. In addition, the target chamber, adjacent beam pipe and cooling trap were baked out (several hours at ≈ 100 ^0C) prior to each measurement.

The targets were mounted in a target holder in which the incoming cooling water is directed towards the rear face of the backing, which gives good cooling of the beam spot.

The γ-ray spectra were measured with Ge(Li) detectors of 100, 95 and 80 cm^3 with a resolution of 2.2, 1.95 and 1.8 keV for the 1.33 MeV ^{60}Co line, respectively. The efficiency curves of the detectors were determined by means of radioactive sources and (p,γ) reactions producing γ-rays of known relative intensities. For some special measurements the 80 cm^3 detector was placed in a NaI shield to obtain Compton-suppressed spectra [26].

The spectra were accumulated in the memory of a PDP 11/34 computer

---

[†] The 0.3 mm thick Ta sheets were obtained from Drijfhout, Amsterdam. The Ta sheets from several other firms proved to be considerably more contaminated with F and Na.

by means of a home-made DMI interface. A CAMAC system connected to this computer was used for computer control of the experiments.

3. Excitation curve

In order to locate the resonances, a reaction yield curve was measured over the range E_p = 0.5 - 2.0 MeV. The upper boundary of this range is 20 keV above the neutron threshold. The proton energies were calibrated with $^{27}Al(p,\gamma)^{28}Si$ resonances, whereas absolute resonance strengths were measured by comparing the strength of a $^{36}S(p,\gamma)^{37}Cl$ resonance with resonances of known absolute strength in $^{32}S(p,\gamma)^{33}Cl$ and $^{34}S(p,\gamma)^{35}Cl$.

3.1. YIELD MEASUREMENT

The reaction yield curve (fig. 1) was measured in steps of 0.1 - 1 keV with three Ge(Li) detectors placed at angles θ = 55°, 125° and -55° with respect to the incident beam direction. At each proton-energy setting, γ-ray spectra were accumulated for a total charge of 300 μC (600 μC for E_p < 600 keV) deposited on the target, and then stored on magnetic tape. During these measurements the beam current was kept between 10 and 15 μA. The influence of electron emission was minimized by applying to the target a potential of +180 V with respect to its surroundings.

Two targets were used in the measurement of the entire yield curve and their condition was monitored by regularly checking the yield of the $^{34}S(p,\gamma)^{35}Cl$ resonance at E_p = 1211 keV which is one of the stronger resonances, even with the highly enriched ^{36}S target material used here. After each check measurement of the 1211 keV resonance, the

Fig. 1. Gamma-ray yield curve of the $^{36}S(p,\gamma)^{37}Cl$ *reaction for* $E_p = 500 - 2000$ *keV. The target thickness was about 10* $\mu g/cm^2$ *Ag_2S (81 % ^{36}S).*

last $^{36}S(p,\gamma)^{37}Cl$ resonance was remeasured. In this way the effects of beam spot changes could be determined, as machine adjustments were made only at these check points.

At proton energies below 1 MeV a shorting rod assembly was used short-circuiting the lower sections of the accelerator, and thus leading to better focussing of the beam.

The data were analysed off-line by integrating over windows set on the spectra. The window limits could be continuously adjusted to changes in excitation energy and Doppler shift. In this way the yield of primary as well as secondary transitions was deduced, after proper background subtraction. Fig. 2 shows an example of two yield curves obtained in this way.
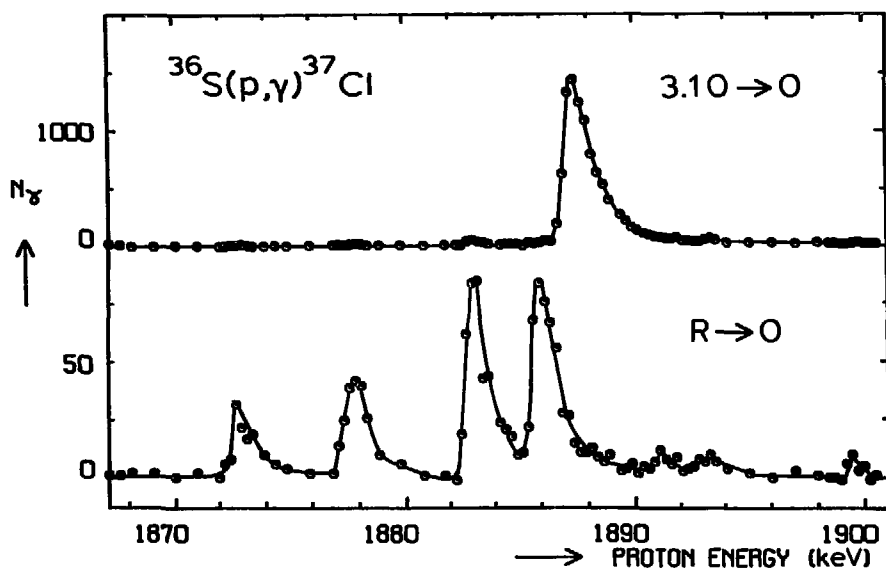
Fig. 2. Yield curves for the $r \to 0$ and $3.10 \to 0$ MeV transitions in the range $E_p = 1870 - 1900$ keV. Background under the peaks in the γ-ray spectrum has been subtracted. The Ge(Li) detector of 80 cm^3 subtended a solid angle of $\Omega = 2$ sr. The accumulated charge is 300 μC per measuring point.

3.2. RESONANCE ENERGIES

The necessity of monitoring the target condition during the yield measurements by periodically checking the yield of the 1211 keV resonance, implies that an effect due to the hysteresis of the analyzing magnet is introduced. This effect was kept small by using only one half of the hysteresis curve, i.e. during the complete yield curve measurements the magnet current was always decreased [see also ref.[6]]. To further reduce the error not one but several ^{27}Al resonances were used for calibration. These well-known [6] resonances were measured "simultaneously" with neighbouring ^{36}S$(p,\gamma)^{37}$Cl resonances in the following way. A special target was prepared, of which the upper half consists of ^{27}Al and the lower half of Ag$_2$^{36}S. With a two-hole diaphragm and a vertical bending magnet, which switches the beam from one hole to the other, the yield of both reactions could be measured sequentially at each proton-energy setting. The proton energy was varied by changing the target voltage from +200 to +6000 V, keeping the analyzing magnetic field and all other machine settings constant. In this way all effects due to changing beam properties are avoided. Both the target current and the actual target voltage were measured [*]. Computer control of the bending magnet and the target voltage made it possible to apply this accurate method. The resonance energies thus obtained (see table 1 and fig.3) served as secondary calibration standards for the yield curve.

The energies of the 187 observed resonances are listed in column 1 of table 2. Many of these have not been reported previously. This is

---

[*] Due to the rather high impedance of the high-voltage power supply in reverse direction, beam current changes result in changes in the target voltage. Only by sampling the voltage during the actual measurements, this effect can be taken into account.

Table 1

Proton energies (in keV) used for calibration

$^{27}Al(p,\gamma)^{28}Si$ [a]	$^{36}S(p,\gamma)^{37}Cl$ [b]
679.30 ± 0.04	678.40 ± 0.11
991.88 ± 0.04	996.22 ± 0.19
1 799.75 ± 0.09	1 799.85 ± 0.12

[a] Ref.[5].　　[b] This work.
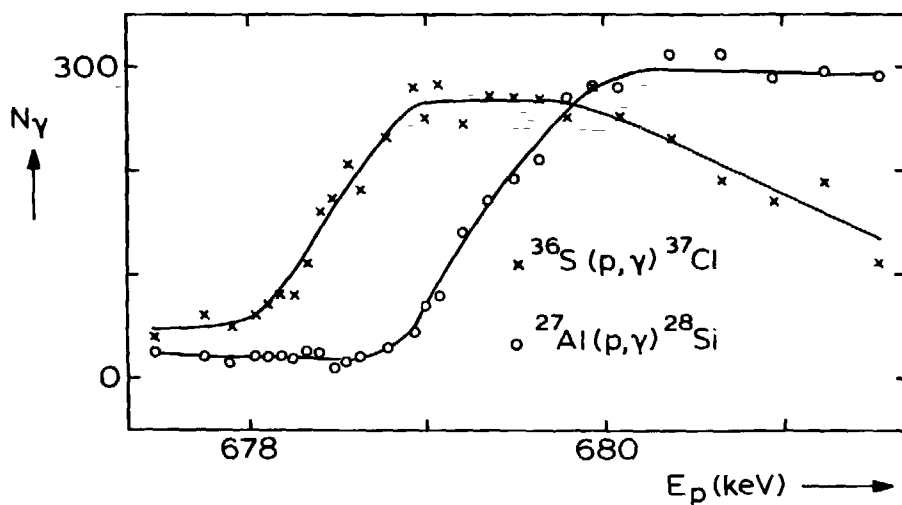
Fig. 3. Simultaneously measured yield curves of the $^{27}Al(p,\gamma)^{28}Si$ and $^{36}S(p,\gamma)^{37}Cl$ reactions around E_p = 679 keV.

only partly due to the fact that hitherto unexplored proton energy ranges have been studied, viz. E_p = 0.5 - 0.8 MeV and E_p = 1.9 - 2.0 MeV. Also in the previously studied range E_p = 0.8 - 1.9 MeV, new resonances were found and multiplets were resolved. This is due to the availability of highly enriched ^{36}S and to the good energy resolution of the Utrecht 3 MV Van de Graaff accelerator.

The resonances reported by Hyder et al.[1] and Piiparinen et al.[2] are also listed in table 2 for comparison. In general the energies agree within the experimental errors.

$^{36}S(p,\gamma)^{37}Cl$ 10 µg/cm^2 Ag$_2$S

Cl YIELD

PROTON ENERGY (keV)
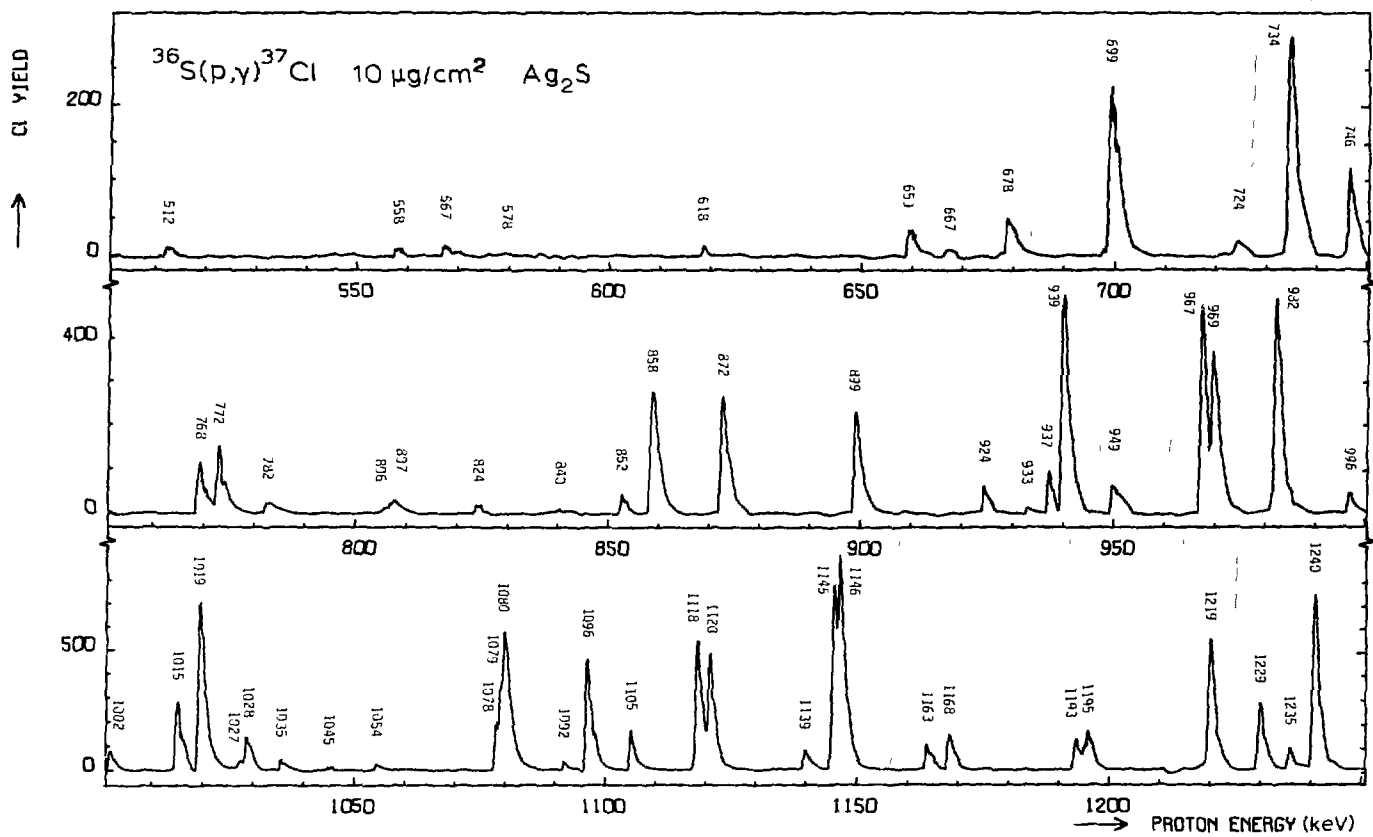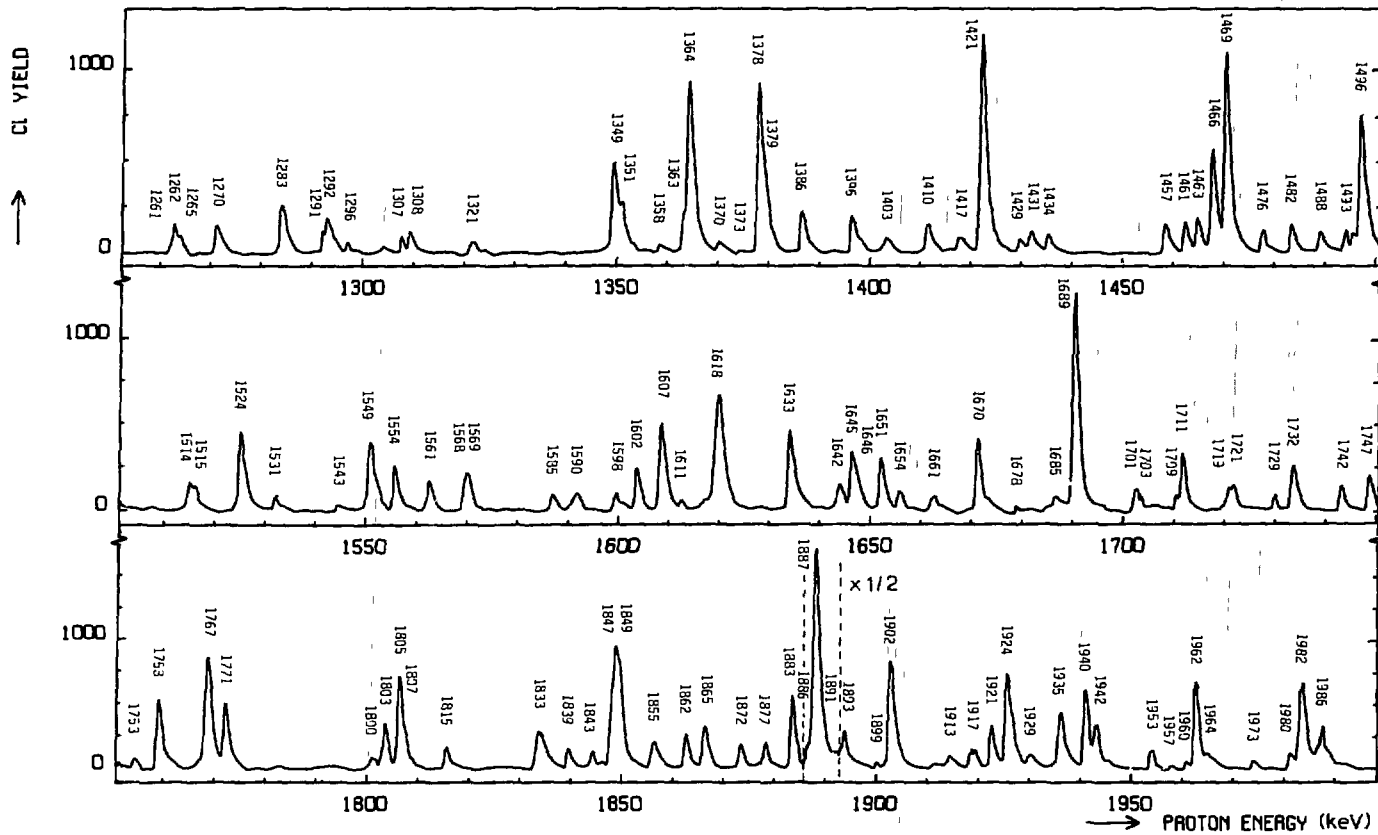
Fig. 4. Reaction yield curve of the reaction $^{36}S(p,\gamma)^{37}Cl$ in the range E_p = 500 – 2000 keV, showing the production rate of ^{37}Cl (in relative units) with a target of 10 μg/cm² Ag_2S. The curve is based on the same data as fig. 1, but note that e.g. the E_p = 1211 keV, $^{34}S(p,\gamma)^{35}Cl$ resonance which produces a large peak in fig. 1 has disappeared completely in this curve.

Table 2
Resonances in the reaction $^{36}S(p,\gamma)^{37}Cl$

	This work		Hyder et al. [1]		Piiparinen et al. [2]
E_p (keV)	E_x (keV) [a]	S (eV) [b]	E_p (keV) [c]	S (eV) [b,d]	E_p (keV) [e]
512 1 ± 0.4	8 884.6	0.032 ± 0.006			
55. 0.4	8 928.9	0.020 ± 0.004			
567.3 ± 0.4	8 938.3	0.046 ± 0.009			
579 . 0 2	8 949.0	0.0070± 0.0014			
618.3 ± 0.2	8 987.9	0.018 ± 0.006			
658.7 ± 0.2	9 027.2	0.12 ± 0.02			
666.6 ± 0.2	9 034.8	0.038 ± 0.009			
678.4 ± 0.2	9 046.4	0.17 ± 0.10			
698.7 ± 0.2	9 066.2	0.82 ± 0 13			
724.C ~ 0.3	9 090.8	0.14 ± 0.04			
734.0 ± 0.2	9 100.5	0.94 ± 0.15			
746.2 ± 0.2	9 112 3	0.30 ± 0.05			
768.4 ± 0.2	9 134.0	0.40 ± 0.07			
772.3 ± 0.2	9 137.8	0.49 ± 0.08			
782.1 ± 0.2	9 147.3	0.062 ± 0.012			
805.6 ± 0.2	9 170.2	}0.078 ± 0.016	805	0.05	
806.5 ± 0.2	9 171.0				
823.6 ± 0.2	9 187.7	0.043 ± 0.009			
839.8 ± 0.2	9 203.4	}0.014 ± 0.005			
845.4 ± 0.2	9 208.9				
852.2 ± 0.2	9 215.5	0.11 ± 0.02			
857.9 ± 0.2	9 221.1	0.83 ± 0.13	860	0.3	
872.0 ± 0 2	9 234.8	0.85 ± 0.14	875	0.8	
898.6 ± 0.2	9 260.7	0.81 ± 0.16	899	0.7	
924.0 ± 0.2	9 285.4	0.22 ± 0.04			
932.6 ± 0.2	9 293.7	0.062 ± 0.015			
936.7 ± 0.2	9 297.7	0.25 ± 0.05			
939.4 ± 0.2	9 300.4	2.0 ± 0.3	940	0.7	
949.3 ± 0.2	9 310.0	0 26 ± 0.05	950	0.1	
966.9 ± 0.2	9 327.1	1.4 ± 0.2	969	0.6	
969.2 ± 0.2	9 329.3	1.7 ± 0.3			
981.5 · 0.2	9 341.3	1.6 ± 0.3	983	0 7	
996.2 ± 0.2	9 355.6	0.18 ± 0.05			
1 001.5 ± 0.2	9 360.8	0.19 ± 0.05			
1 014.5 ± 0.2	9 373.4	0.9 ± 0.2			1 016
1 019.0 ± 0.2	9 377 8	1.5 ± 0.3	1 020	1 3	1 020
1 027.0 ± 0.2	9 385.6	0.09 ± 0.03			
1 028.4 ± 0.2	9 386.9	0.64 ± 0.14			1 029
1 035.2 ± 0.2	9 393.6	0.21 ± 0.05			1 036
1 044.9 ± 0.2	9 403.0	0.11 ± 0.03			
1 054.2 ± 0.2	9 412.0	0.10 ± 0.02	1 055	0.3	
1 077.9 ± 0.2	9 435 1	}3.4 ± 0.6			
1 078.8 ± 0.2	9 436.0		1 079	1.3	1 080
1 079.5 ± 0.2	9 436.7				
1 091.6 ± 0.2	9 448.4	0.19 ± 0.04			1 093
1 096.0 ± 0.2	9 452.7	1.7 ± 0.3	1 096	0.7	1 097
1 104 6 ± 0.2	9 461.1	0.9 ± 0.2	1 105	0.6	1 106
1 117.6 ± 0.2	9 473.7	2.0 ± 0.5			1 119
1 120.1 ± 0.2	9 476.2	1.8 ± 0.5	1 120	1.3	1 121
1 139.3 ± 0.2	9 494.8	0.43 ± 0.09	1 140	0.3	1 140
1 144.9 ± 0.2	9 500.3	}5.2 ± 1 0	1 147	1.7	1 146
1 146.0 ± 0.2	9 501.4				
1 163.4 ± 0.2	9 518.3	0.43 ± 0.08	1 164	0.4	1 164
1 167.5 ± 0.2	9 522.3	0.72 ± 0.13	1 167	0.5	1 168
1 192.8 ± 0.2	9 546.9	0.41 ± 0.07			1 193
1 194.6 ± 0.2	9 548.7	}1 03 ± 0.16			
1 195.3 ± 0.2	9 549.3		1 195	1 1	1.196
1 219.2 ± 0.2	9 572.6	2.1 ± 0.3	1 221	1.3	1 220
1 229.0 ± 0.2	9 582.1	1.4 ± 0.3	1 225	1 0	1 231
1 235.0 ± 0.2	9 588.0	0.43 ± 0.10	1 230	0.8	1 236
1 239.8 ± 0.2	9 592.6	3.5 ± 0.8	1 241	1.3	1 240
1 261.3 ± 0.2	9 613.6				
1 262.1 ± 0.2	9 614.4	}0.77 ± 0.17	1 265	1.1	1 262
1 264.6 · 0.2	9 616.8				
1 270.2 ± 0.2	9 622.2	0.77 ± 0.17	1 272	0.4	1 271

This work			Hyder et al. [1]		Piiparinen et al. [2]
E_p (keV)	E_x (keV) [a]	S (eV) [b]	E_p (keV) [c]	S (eV) [b,d]	E_p (keV) [e]
1 283.0 ± 0.2	9 634.7	1.3 ± 0.3	1 284	1.0	1 284
1 291.3 ± 0.2	9 642.7	}1.2 ± 0.3	1 293	0.4	1 293
1 292.1 ± 0.2	9 643.5				
1 296.2 ± 0.2	9 647.5	0.21 ± 0.05			1 297
1 306.8 ± 0.3	9 657.8	0.25 ± 0.06	1 303	0 3	
1 308.4 ± 0.3	9 659.4	0.36 ± 0.11	1 310	0.3	1 309
1 320.5 ± 0.3	9 671.5	}0.21 ± 0.07	1 322	0.8	1 322
1 320.9 ± 0.3	9 671.6				
1 348.8 ± 0.3	9 698.7	1.6 ± 0.4			1 350
1 350.6 ± 0.3	9 700.4	1.3 ± 0.3	1 352	1.7	1 352
1 358.0 ± 0.3	9 707.6	0.15 ± 0.05			
1 362.8 ± 0.3	9 712 3	}4.8 ± 1.1	1 366	2.3	1 365
1 363.7 ± 0.3	9 713.2				
1 369.7 ± 0.3	9 719.0	}0.26 ± 0.07			
1 373 4 ± 0.3	9 722.6				
1 377.6 ± 0.3	9 726 7	}4.6 ± 1.0	1 380	1.7	1 378
1 379.0 ± 0.3	9 728.1				
1 386.2 ± 0.3	9 735.1	1.0 ± 0.2	1 390	0.9	1 388
1 396.1 ± 0.3	9 744 7	1.0 ± 0.2	1 398	1.3	1 397
1 402.9 ± 0.3	9 751.6	0.50 ± 0.11	1 404	2.5	1 404
1 410.2 ± 0.3	9 758 4	0.8 ± 0.2			1 412
1 416.6 ± 0 3 [h]	9 764.7	0.76 ± 0.19			1 419
1 420.9 ± 0.3	9 768 8	8.2 ± 1.9	1 424	2.5	1 422
1 428.5 ± 0.3	9 776.2	0.43 ± 0.10			1 425
1 430.5 ± 0.3	9 778.2	0.85 ± 0.19			1 432
1 434.0 ± 0.3	9 781.6	0.61 ± 0.14	1 435	0 4	1 436
1 457.0 ± 0.3	9 804 0	1.1 ± 0.3			1 459
1 460.9 ± 0.3	9 807 8	0.9 ± 0.2			1 462
1 463.4 ± 0.3	9 810.2	1 2 ± 0 3	1 461	0 5	1 465
1 466.3 ± 0.3	9 813.0	3.3 ± 0.7			1 468
1 469 0 ± 0.3	9 815.6	7.3 ± 1.6	1 471	2 9	1 470
1 476.1 ± 0.3	9 822.5	0.81 ± 0.19			1 478
1 481.9 ± 0.3	9 828 2	1 1 ± 0.3	1 480	1 0	1 483
1 487.6 ± 0.3	9 833.7	0.83 ± 0.18	1 498	0.4	1 489
1 492.5 ± 0.3	9 838.5	0.50 ± 0.12			
1 495.6 ± 0.2	9 841.4	6.0 ± 1.4	1 497	1 8	1 496
1 500.1 ± 0.3	9 845.9	0.51 ± 0.14	1 000	2 0	1 501
1 513.5 ± 0.3	9 858.8	0.51 ± 0.14			
1 514.6 ± 0.3	9 859.9	1.9 ± 0.4	1 514	1 6	1 515
1 523.6 ± 0 3	9 868.7	3.6 ± 0.8	1 522	1 2	1 523
1 530.6 ± 0 3	9 875 5	0.56 ± 0.13	1 529	0 2	1 530
1 543.3 ± 0.3	9 887 8	0.36 ± 0 09	1 542	0.4	1 544
1 549.2 ± 0.3	9 893.6	3.2 ± 0.7	1 548	1 0	1 550
1 554.2 ± 0.3	9 898.4	1.9 ± 0.4	1 553	1 2	1 555
1 560.8 ± 0.3	9 904.9	}1.2 ± 0 3	1 559	0 5	1 561
1 568.0 ± 0 3	9 911.9				
1 568.8 ± 0.3	9 912.6	2.1 ± 0.5	1 569	0.7	1 569
1 585.3 ± 0.3	9 928.8	0.58 ± 0 13			1 584
1 589.6 ± 0.3	9 932.9	0 83 ± 0.19	1 589	0.4	1 590
1 597.7 ± 0.3	9 940.8	0.67 ± 0.15			1 598
1 602.0 ± 0.3	9 945.0	1.4 ± 0.3	1 603	0 6	1 603
1 606.8 ± 0.2	9 949.7	3.5 ± 0.8	1 608	1.4	1 607
1 611.2 ± 0.3	9 954.0	0.17 ± 0.09			1 612
1 618.0 ± 0.2 [g]	9 960.6	7.2 ± 1.6	1 619	2.0	1 618
1 632.5 ± 0.2	9 974.2	3.6 ± 0.8	1 632	1.1	1 633
1 642.2 ± 0.2	9 984 1	}1 1 ± 0.3	1 643	1.3	1 643
1 644.7 ± 0.2	9 986.6				
1 645.7 ± 0.2	9 987.5	3.1 ± 0.7	1 646	1.7	1 646
1 650.7 ± 0.2	9 992.3	1.8 ± 0.4	1 651	0.9	1 651
1 654.3 ± 0.2	9 995.9	1.0 ± 0.2	1 653	0.7	1 654
1 660.7 ± 0.2 [h]	10 002.1	0.85 ± 0.19	1 662	0.9	1 661
1 669.7 ± 0.2	10 010.9	3.0 ± 0.6	1 670	1 5	1 670
1 677.5 ± 0.2	10 018.5	0.18 ± 0.06			1 678
1 685.2 ± 0.2	10 025.0	0.80 ± 0.18			1 686
1 689.0 ± 0.2	10 029.7	7 ± 2	1 691	2.3	1 690

This work			Hyder et al. [1]		Piiparinen et al [2]
E_p (keV)	E_x (keV) [a]	S (eV) [b]	E_p (keV) [c]	S (eV) [b,d]	E_p (keV) [e]
1 701.0 ± 0.2	10 041.3	⎫0.7 + 0.2			1 702
1 702.8 ± 0.2	10 043.1	⎭			
1 709.2 ± 0.2	10 049.3	0 23 ± 0.07			1 705
1 710.5 ± 0.2	10 050.6	1.8 ± 0.5	1 711	0 8	1 710
1 719.3 ± 0.2	10 059.2	0.33 + 0.09			
1 720.6 ± 0.2	10 060.4	1.0 ± 0.3	1 721	1.2	1 721
1 728.8 ± 0.2	10 068.4	0.38 ± 0.10			1 729
1 732.2 + 0.2	10 071.7	1.9 + 0.5	1 732	1.?	1 733
1 741.8 ± 0.2	10 081.1	0.9 + 0.2			
1 74ა.0 ± 0.2	10 085.2	0.14 ± 0.05			
1 747.4 ± 0.2	10 086.5	1.2 ± 0.3			
1 753.3 ± 0.2 [h]	10 092.3	0.56 ± 0.14			
1 757.9 ± 0.2	10 096.7	3.4 ± 0.8	1 756	1.6	1 758
1 765.3 ± 0.3	10 104.0	0.4 + 0.2			1 763
1 767.2 + 0.2	10 105.8	6.8 + 1.5	1 767	2.8	1 767
1 770.9 ± 0.2	10 109.4	3.7 ± 0.8	1 770	1.3	1 771
1 799.8 ± 0.2	10 137.6	0.80 ± 0.19			
1 802.6 ± 0.3	10 140.2	2.7 ± 0.6	1 803	2.8	1 803
1 805.3 ± 0.3	10 142.8	⎫6.2 ± 1.3	1 806	2 7	1 805
1 806.9 ± 0.3	10 144.4	⎭			
1 814.5 ± 0.3	10 151.8	1.6 ± 0.4	1 814	0.9	1 815
1 832.5 ± 0.3	10 169.3	3.7 ± 0.8			1 832
1 838.6 ± 0.3	10 175 2	1 1 ± 0 2			1 837
1 843.4 ± 0.3	10 179.9	1 02 ± 0 17			1 843
1 847.1 ± 0 3	10 183 5	⎫10.0 ± 1 6			1 847
1 848.5 ± 0.3	10 184.9	⎭			
1 855.1 ± 0.3	10 191.3	2.0 ± 0.3			1 855
1 861.6 ± 0.3	10 197.6	⎫1.6 ± 0.3			1 862
1 865.1 ± 0.3	10 201 0	⎭			
1 865.8 ± 0.3	10 201 7	3.5 ± 0.6			1 865
1 872.4 ± 0.3	10 208 1	1.9 ± 0.3			1 872
1 877.2 ± 0.3	10 212 8	1.6 ± 0 3			1 878
1 882.6 ± С.3	10 218 1	4.2 + 0.7			1 882
1 885.5 ± 0.3	10 220.9	2.3 + 0 4			
1 886.9 ± 0.3	10 222.2	32 ± 3	1 889	27 [f]	1 887
1 890.9 ± 0.3	10 226.1	2.5 ± 0.4			
1 892.8 ± 0.3	10 228.0	2.7 ± 0 4			
1 899.0 ± 0.3	10 234 0	0.29 + 0 07			
1 901.5 ± 0.3	10 236.4	6.9 ± 1 1			1 901
1 913.3 ± 0.3	10 247.9	0.88 ± 0.15			
1 917.2 ± 0.3 [g]	10 251.7	1.5 ± 0 3			
1 921.3 ± 0.3	10 255.7	1.9 ± 0.3			
1 924.3 ± 0.3	10 258 6	5.2 ± 0.8			
1 928.9 ± 0.3	10 263.1	1.3 ± 0.2			
1 934.8 ± 0.3	10 268 8	4.0 ± 0.6			
1 939.7 ± 0.3	10 273 6	3.2 ± 0.5			
1 941.8 ± 0.3	10 275.7	4.7 ± 0.8			
1 952.6 ± 0.3	10 286.3	1.6 ± 0.3			
1 956.7 ± 0.3	10 290.2	0.23 ± 0 05			
1 959.7 ± 0.3	10 293.1	0.36 ± 0.07			
1 961.6 ± 0.3	10 294.9	4.2 ± 0.7			
1 964.0 ± 0.3	10 297.3	1.3 ± 0.2			
1 972.6 ± 0.3	10 305.6	0 83 ± 0.16			
1 975.5 ± 0.3	10 308.3	0.21 ± 0.06			
1 979.9 ± 0.3	10 312.7	1.01 ± 0.19			
1 982.1 ± 0.3	10 314.9	5.9 ± 0.9			
1 986.0 ± 0.3 [g]	10 318.7	3 7 ± 0.6			

[a] Calculated with the Q-value Q = 8 386.3 ± 0.2 keV.

[b] $S = (2J+1)\Gamma_p\Gamma_\gamma/\Gamma$.

[c] All ± 3 keV.

[d] Strengths of ref.[1] renormalized on S = 9.7 eV for the E_p = 1 211 keV resonance in $^{34}S(p,\gamma)^{35}Cl$. Strengths are estimated to be valid with at best a factor of 2.

[e] All ± 2 keV.   [f] Ref. [3].

[g] Doublet.   [h] Possibly doublet.

3.3. RESONANCE STRENGTHS

The *relative* resonance strengths were determined from the areas of the resonance peaks in the background corrected yield curves of the r → 0, 1.73 → 0, 3.09 → 0 and 3.10 → 0 MeV transitions. The latter three transitions can be regarded as the "drains" through which most of the cascading decay of the resonance level will proceed; the three lowest excited states have spins J = 1/2, 5/2 and 7/2, the ground state J = 3/2. The sum ΣN_d of the intensities (corrected for the detector efficiency) of the four transitions mentioned, therefore will be to a good approximation proportional to the total number N_γ of ^{37}Cl nuclei decaying by γ-ray emission. In fig. 4 this sum ΣN_d is plotted as a function of the proton energy. A quantitative estimate of the quality of this approximation can be deduced from the 75 resonances of which the γ-ray decay has been measured in some detail (see also sect. 4.2). There the ratio $N_\gamma/\Sigma N_d$ ranges from 1.0 to 1.5 with an average of 1.3. This factor has been used to calculate N_γ for the 112 resonances of which the decay scheme is not available. For the other 75 resonances the measured factor was used.

The expression for the resonance strength as deduced from a thin-target yield curve [see e.g. Gove [25)]], reduces for the present experiment to the simple relation

$$S \propto E_p A$$

where A is the area of the resonance peak in fig. 4. This curve thus gives a better representation of the relative resonance strength than the conventional yield curve (fig. 1). In addition, the new method of analyzing the yield of single transitions, although it reduces the sensitivity, considerably improves the discrimination against contaminant resonances. A good example in this respect is the $^{34}S(p,\gamma)^{35}Cl$

Table 3

Resonances used for strength calibration

Reaction	E_p (keV)	Analyzed transition	E_γ (MeV)	Branching ratio	Ref.
$^{32}S(p,\gamma)^{33}Cl$	587	$r \to 0$	2.85	0.45	8
		$r \to 0.81$	2.04	0.55	
$^{34}S(p,\gamma)^{35}Cl$	1 211	$3.16 \to 0$	3.16	0.88	9,10
$^{36}S(p,\gamma)^{37}Cl$	1 887	$3.10 \to 0$	3.10	0.87	a

[a] Present work; branching ratio refers to all ground state decay instead of all primary decay (see also section 4.2).

resonance at E_p = 1211 keV. In a conventional yield curve (fig. 1) it is one of the stronger resonances, but in the new yield curve (fig. 4) this contaminant disappeares completely.

Absolute strengths were deduced from the relative strengths thus obtained, by normalization to the strength of the E_p = 1887 keV, J^π = 7/2⁻ resonance. The strength of this resonance was compared to the well-known strength of $^{32}S(p,\gamma)^{33}Cl$ and $^{34}S(p,\gamma)^{35}Cl$ resonances in a separate experiment with targets of moderately enriched ^{36}S [*]. The yield was measured of selected transitions in the resonances at E_p = 587 keV (^{32}S), E_p = 1211 keV (^{34}S) and E_p = 1887 keV (^{36}S). The transitions selected and their branching ratios are given in table 3. To minimize the influence of efficiency errors, two precautions were

[*] Obtained from Oak Ridge National Laboratory, U.S.A.
Composition: 3.51 % ^{36}S, 5.45 % ^{34}S, 0.95 % ^{33}S, 90.1 % ^{32}S.

taken: (i) the efficiency was measured in exactly the same set-up, with a ^{56}Co-source at the position of the beam spot (the target was replaced by a bare backing); (ii) decay lines with roughly equal γ-ray energy were used. Extreme care was taken to minimize the effects of beam-spot changes on a (probably) inhomogeneous target. Especially when resonances of different energy are compared, the effects of the changing focussing properties of the accelerator can be quite large: in preliminary measurements the ratio of the strength of the 587 and 1211 keV resonances changed up to 40 % in different experiments. These effects were reduced by placing, close to the target, a diaphragm with a hole smaller than the beam diameter. Background radiation from this Ta diaphragm was minimized by heating it to incandescence by the proton beam prior to the measurements.

Table 4 lists two strength ratios determined in the present experiment and the ratios and absolute strengths found in the literature [refs.[11-14]]. A least-squares fit of these quantities leads to the values for the ^{32}S(p,γ)^{33}Cl, ^{34}S(p,γ)^{35}Cl and ^{36}S(p,γ)^{37}Cl resonance strengths also listed in table 4.

The resonance strengths thus obtained are listed in column 3 of table 2. The final errors are due to: (i) The statistical error in the area A. (ii) The 9 % error in the strength of the 1887 keV ^{36}S(p,γ)^{37}Cl resonance used for normalization. (iii) An error due to the target deterioration and beam spot changes during the measurement of the yield curve. The size of these effects was estimated by the measurements at each check point. The effects were considered to be zero at the beginning of each interval, increasing linearly with proton energy. Half of the effect measured over the relevant 100 keV interval was adopted for this error. (iv) An error due to the effect of beam spot changes caused by the gradually changing focussing properties of the accelerator.

Table 4

Relative and absolute strengths of the E_p = 587, 1211 and 1887 keV resonances in the reactions $^{32}S(p,\gamma)^{33}Cl$, $^{34}S(p,\gamma)^{35}Cl$ and $^{36}S(p,\gamma)^{37}Cl$, respectively

	Input data		Results of least-squares analysis
	this work	other work	
$S(^{32}S)/S(^{34}S)$	0.023 ± 0.003	0.017 ± 0.003 [a,f]	-
$S(^{34}S)/S(^{36}S)$	0.27 ± 0.03	0.36 [b,f]	-
$S(^{32}S)$	-	0.21 ± 0.03 eV [c]	0.22 ± 0.03 eV
$S(^{34}S)$	-	9.4 ± 0.5 eV [d]	9.4 ± 0.5 eV
$S(^{36}S)$	-	22 ± 3 eV [e,f]	33 ± 3 eV

[a] Aléonard et al.[11].
[b] Calculated from the strengths given by Harris et al.[3].
[c] Adopted value from the review by Endt [14].
[d] Weighted average of the values from refs.[4,11-13].
[e] Keinonen et al.[4].
[f] Not used in the present analysis; given for comparison only.

This effect is only partly taken into account by the check-point measurements. This error increases linearly with the energy difference from zero at the 1887 keV calibration resonance to 10 % at E_p = 500 keV.
(v) An error of 15 % due to the uncertainty in the decay of those resonances of which the decay was not measured.

In order to facilitate comparison, the resonance strengths reported by Hyder et al.[1] and listed in table 2, have been renormalized to the new value of the strength of the E_p = 1211 keV $^{34}S(p,\gamma)^{35}Cl$ resonance. Hyder's values then deviate from the present strengths up to a factor of two in both directions. This factor of two is indeed the uncertainty quoted in ref.[1].

In addition to those listed in table 2, Hyder et al.[1] also reported resonances at E_p = 830, 1154, 1449, 1581 and 1817 keV. We determine upper limits for the strengths of these resonances of S = 0.005, 0.04, 0.1, 0.07 and 0.05 eV, respectively, to be compared with Hyder's values of S = 0.1, 0.4, 0.38, 0.2 and 1.0 eV. The ratio of these strengths might indicate that these five resonances are due to target contaminations.

The paper of Piiparinen et al.[2] does not quote resonance strengths. The $^{36}S(p,\gamma)^{37}Cl$ resonances at E_p = 1099, 1211, 1215, 1518 and 1587 keV, listed in this paper, have not been found in the present experiment. From our yield curve we deduce upper limits for the strength of eventual $^{36}S(p,\gamma)^{37}Cl$ resonances at these energies of S = 0.03, 0.04, 0.08, 0.06 and 0.04 eV, respectively. The relative strengths of the resonances as indicated by the yield curve of ref.[2], suggest that these resonances are also due to contaminants.

3.4. MULTIPLETS AND RESONANCE WIDTHS

In order to locate close multiplets, the apparent resonance widths (FWHM) were plotted as a function of E_p (fig. 5a). The resonances at E_p = 1416, 1618, 1661, 1753, 1917 and 1986 keV show an appreciable width. Detailed comparison of the yield curves for different γ-ray energy windows definitely proves the doublet character of the E_p = 1618 (see fig. 6), 1917 and 1986 keV resonances; at the E_p = 1416, 1661 and 1753 keV resonances there is no direct evidence for a doublet structure.

The interquartile range of the low-energy side of the resonance peaks can yield information on the natural width of the resonances. The interquartile range of the stronger resonances is plotted in fig. 5b. The resonances at E_p = 1416 and 1661 keV again show up; the widths deduced from the measured interquartile ranges are Γ = 0.5 $\pm$ 0.1 and 0.4 $\pm$ 0.1 keV, respectively. For the natural width of all the remaining observed singlet resonances one finds [23] an upper limit (corresponding to two standard deviations) of Γ < 0.4 keV. From the data of fig. 5a one
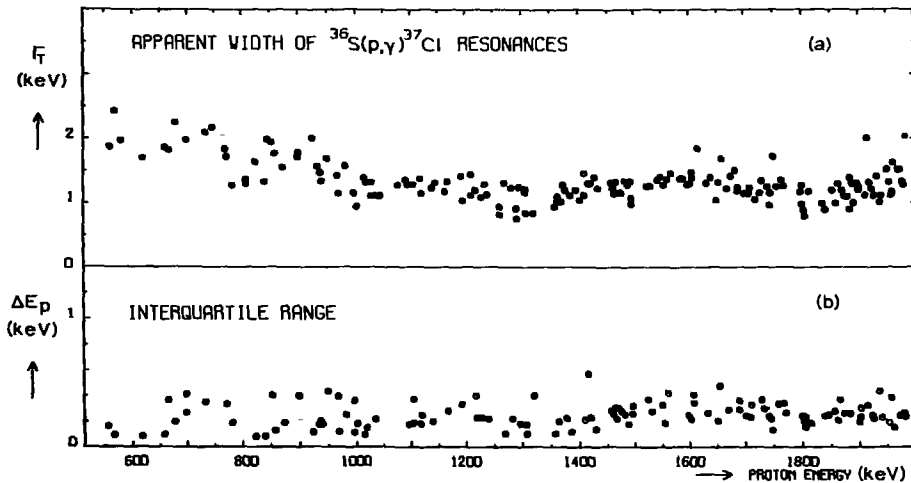
Fig. 5. Apparent width Γ_T and interquartile range ΔE_p of singlet resonances in $^{36}S(p,\gamma)^{37}Cl$ in the range E_p = 500 – 2000 keV.

finds [24] $\Gamma < 0.8$ keV. For the presently used targets the interquartile ranges are obviously a more sensitive measure for the determination of Γ than the widths of the resonance peaks; the latter are useful for the identification of doublets.
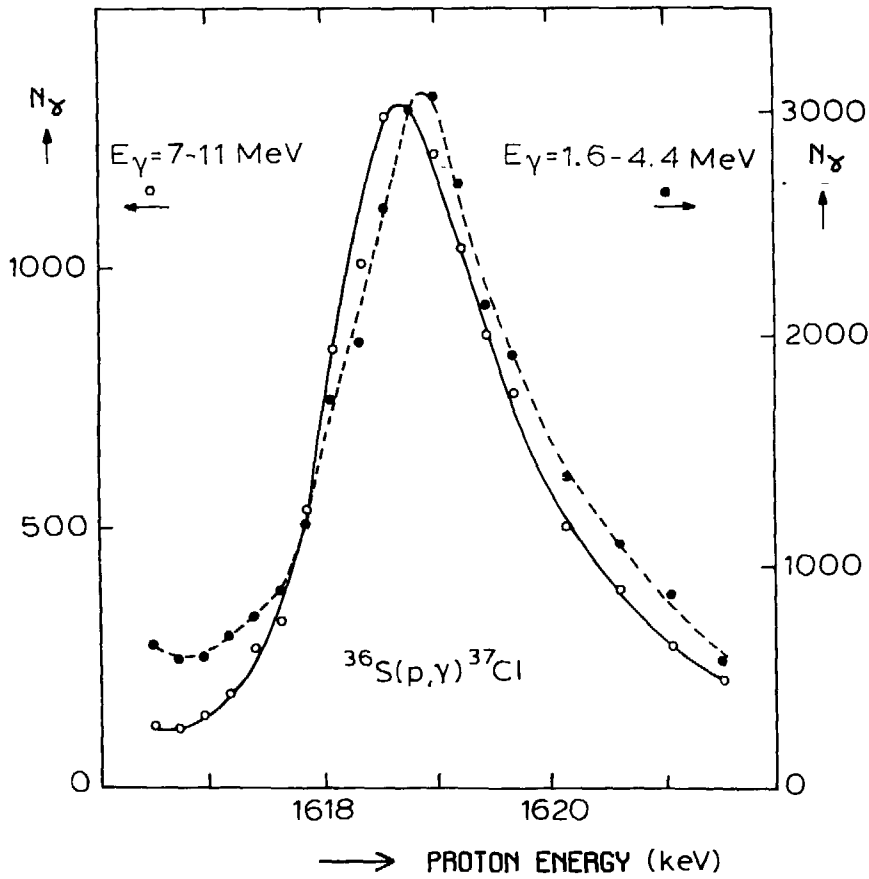
Fig. 6. The yield curves for the γ-ray energy windows $E_\gamma = 1.6 - 4.4$ MeV and $E_\gamma = 7 - 11$ MeV showing the doublet structure at $E_p = 1618$ keV. Target thickness 10 $\mu g/cm^2$ Ag_2S.

3.5. REACTION Q-VALUE

The reaction Q-value was deduced from measurements at the E_p = 996 keV resonance. The proton energy of this resonance was determined with an uncertainty of 0.2 keV, as discussed in sect. 3.2, whereas the necessary γ-ray energies were measured in a separate experiment, analogous to the one described by Alkemade et al.[15]. The well-known [17] γ-ray energies of E_γ = 4 461 240 $\pm$ 19 eV and E_γ = 4 806 055 $\pm$ 22 eV from a ^{66}Ga source [*] were used to calibrate the r $\rightarrow$ 4.84 MeV (E_γ = 4.52 MeV) transition and the 4.84 $\rightarrow$ 0 MeV transition in the following way. The source is placed on the line connecting the beam spot and the centre of the detector, as close as possible to the target, in order to prevent energy shifts due to different detection geometries [for a further discussion, see Helmer et al.[16]]. Doppler-shift effects are eliminated by measuring alternately at two angles, θ = +90^0 and θ = -90^0.

A special alignment procedure guarantees that the two detector positions and the beam spot form one straight line. In this way the effects of small deviations of the measuring angles from θ = +90^0 and -90^0 will cancel. The target is placed alternately at ϕ = +45^0 and ϕ = -45^0 to compensate for the influence of beam spot shifts.

In the analysis the peak positions were determined from the centre-of-gravity of the peaks rather than from the Gaussian fit to eliminate effects due to the difference in line shape of "source" and "reaction" lines. After correction for nuclear recoil the excitation energy of the resonance was obtained as E_x = 9355.64 $\pm$ 0.12 keV. Combined with the proton energy E_p = 996.22 $\pm$ 0.19 keV this gives Q = 8386.34 $\pm$ 0.23 keV, to be compared with the value of Q = 8384.8 $\pm$ 1.5 keV given in Wapstra's most recent evaluation of atomic masses [18].

---

[*] Produced with the Utrecht 6 MV tandem Van de Graaff accelerator in the reaction ^{63}Cu(α,n)^{66}Ga at E_α = 18 MeV.

4. Gamma-ray spectra

4.1. MEASUREMENTS

At 75 resonances in the ranges E_p = 0.5 - 1.2 MeV and E_p = 1.8 - 2.0 MeV, γ-ray spectra were measured at the angles θ = 55° and θ = 90° with respect to the proton beam for a total accumulated charge of 30 - 100 mC. At some especially interesting resonances spectra were measured for a longer time and/or with the Compton suppression spectrometer. The decay modes of the resonance levels and the bound states were determined from the θ = 55° spectra. The 90° spectra served mainly for coarse energy determinations. As an example of the γ-ray spectra, fig. 7 shows a θ = 55° Compton suppressed spectrum measured at the E_p = 1015 keV resonance.

4.2. RESONANCE DECAY

The branching ratios of the resonance states are given in table 5. The quoted branching ratios are relative to the sum of all ground-state transitions, instead of relative to the sum of all primary transitions. In this way the amount of undetected decay can be estimated. The percentage of unknown decay reflects the quality of the data. The relative errors in the branchings vary from a few percent for the strong lines to up to 50 % for the weakest transitions.

As can be seen in figs. 1 and 4, the resonance peaks have a non-negligible tail. This implies that for nearby resonances, lines from the lower-energy resonance may be observed in the spectrum measured at the higher-energy resonance. Some branchings, indicated as such in table 5, have been corrected for the contribution of resonances at lower E_p. In practically all other cases these contributions are small, as can be judged from the relative intensities of transitions that are strong in the decay of the lower energy resonances.

23

Table 5

Gamma-ray branching ratios of resonances in the reaction $^{36}S(p,\gamma)^{37}Cl$

E_p (keV)	E_{x1} (MeV)	E_{x1} J^π :	0 3/2+	1.73 1/2+	3.09 5/2+	3.10 7/2-	3.63 3/2	3.71 3/2+	3.74 5/2-	4.01 9/2-	4.02 3/2+	4.18 3/2	4.269 (1/2)	4.273 7/2-	4.40 (5/2)	4.46 7/2-	4.80 5/2+	4.81 (7/2)	4.84 5/2	4.85 5/2+	4.90 3/2	4.96 3/2	5.01	5.05	5.06	5.23	5.31	5.32	5.37	Other levels, $E_x(f)$	Unknown
512	8.885	3/2+	25																												30
558	8.929		45	45																											25
567	8.938		65																												15
618	8.988		80		30		15														5										10
659	9.027		44	5	12		20	8	10		5	4			3				1			5										15
678	9.047	3/2	54				5	6	3			7	2		2	3						2									5 65[2]	8
699	9.066	3/2	50	3	7		9	8	5		2	11	2			3			1			2		1							5,62[1], 6.36[2], 6 67[1]	10
734	9.101		66	4				1			11	1	2							2											6 32[2]	10
746	9.112		57	8	10		1	2			1	1	2						1	6		7	3	1							5.49[8], 6 42[8]	5
768	9.134		35	2	2		3	4	11		3		9			2						7		1							5 91[3], 6.04[1]	10
772	9.138		65																													8
782	9.147		92																													10
806a	9.171		72	10	2		2	5			7		2		2							2			6					6	5 62[8], 5 92[6], 6 37[4], 6.67[8]	14
824	9.188		11	11	4	12		4	11		7		5							2		8			5					4	5 65[1], 5.94[2], 5.98[5], 6 67[3]	8
840	9.203		49	6	9	12			1		2	2	8						4											4	4 67[1]	15
852	9.216	3/2	44	2	3	1	7				4		3									2	2			3						2
858	9.221		61	11	1		6					9											1	3		1						10
872	9.235		19	41	12			7	3		25	6	4		1				3		3					4				3	5.62[2], 5.94[1], 5.99[1], 6 04[1]	18
899	9.261		16	35				3			10	2							3							1				9	5 02[3], 6.31[3]	8
924	9.285	1/2	18	5			16	19					4						3									10				25
933	9.294		3			12	12	11																							7 08[6]	15
937	9.298		23	3	3	12	11									5			2												5 65[2]	15
939	9.300		44	14	14	1									6									3								6
949	9.310		85	4	5			1			1													1		3				3	5 65[1], 6.42[1]	10
967	9.327		1	72			3	1	4		4			2		2																10
969	9.329		27	27	1	20	3	1	1		4			5		5		1		3				4		2	1			1	5 91[3]	7
982	9.341		47	19		17	13		8		4		1	5			1	16		3		7					2			2		30
996	9.356		7				2		2		4	1		5		2	5	14		3		4									5 49[3], 5 58[1], 6 02[1], 6 37[2]	5
1015	9.373	5/2	18	3	5	12		1			1	1	1			1	1	2					1								5 49[1], 5.65[1], 5 91[1], 5 98[2]	4
1019	9.378		80	22	1	1						2	2					2		1	2	2		2							5 91[4], 6 42[3], 6 49[4], 6 73[1]	7
1028a	9.387		17	9	2		4		1		4	3	2					2		2		2	8		2	6				2	5 94[3], 6.02[3], 6 04[2], 6 37[3]	15
1035	9.394		20	31	2			16	5		1		4		7			3													5 91[2]	20
1080a	9.436		31	15																			2									40
1092	9.448		30	15	15		1		1		3	3			2	2			3		1		3			1				5	5.92[1], 5 98[1], 6 73[1]	6
1096	9.453		68	5			45				2	6			1					2		1								1	5 94[1], 5 98[1], 6 02[2], 6.49[1]	15
1105	9.461	5/2	10		2		3		1		6		5			1				2										2	5 62[1], 5.65[2]	20
1118	9.474		48	9	1	1	1				1		1		4																5 62[1], 6 02[1], 7 15[1]	5
1120	9.476		46	20	6								5									3								2	6 37[2], 6 67[2]	22
1139	9.495		40	3	1				2			2	1			2		1		1											5.65[1], 6 36[1]	10
1145	9.500		45	35								1	2								1											13
1146b	9.501		75	23	5						10		11																	5	5 65[3], 5 59[2], 6 67[2], 7 08[3]	13
1163	9.518		23	24	1		1				30																				5 73[2], 5 94[2], 5 99[6]	20
1168	9.522	5/2	7	3c	10						3				9			2		3	6	3										15
1193	9.547		65				1	3					10																		5 62[1], 5 99[1], 6 02[3], 6 04[2]	6
1219	9.573	1/2	70			5																								3		

Table 5 (continued)

E_0 (keV)	E_{xi} (MeV)	E_{xf} J^π	0 3/2+	1.73 1/2+	3.09 5/2+	3.10 7/2-	3.63 3/2	3.71 3/2+	3.74 5/2-	4.01 9/2-	4.02 3/2+	4.18 3/2	4.269 (1/2)	4.273 7/2-	4.40 (5/2)	4.46 7/2-	4.80 5/2+	4.81 (7/2)	4.84 5/2	4.85 5/2+	4.90	4.96 3/2	5.01	5.05	5.06	5.23	5.31	5.32	5.37	Other levels, E_x(%)	Unknown
1839	10.175		48	6			4				9									3										5.62(7), 5.92(5)	15
1843	10.180		4	2[c]	28	14		9				4			2		7														30
1847	10.183		17	45	16		4		1	1								1													15
1849	10.184		24	22[c]	11		4	3		2	2		5	3		2		2													20
1855	10.191		47	21			2	2	2				4		2																20
1862	10.198		34		21	1	1	1		10			2																		30
1865[a]	10.201		5		1	18	20	1	1	2	1		1	1	4			5	9												5.53(1), 5.57(2), 5.98(3)	25
1872	10.208	3/2	28	3	2		4	13		15	3		2				5			2		1									5.49(2), 5.65(2)	18
1877	10.213		53				9	2		2			2		1	1	6														5.65(1), 5.94(1), 7.25(2)	20
1883	10.218		32		17		1	20	1			1		1		1	2			3			2								5.49(3), 5.65(1), 5.91(2)	13
1886	10.221		64	2	2	6		6	1									3			2										5.49(3), 6.31(1),	10
1887[b]	10.222	7/2-			1	74		1						1	1	4															5.57(4), 5.73(2), 6.35(2)	10
1891[b]	10.226		11		31	3		20		7				2					2												5.49(?), 5.57(2)	20
1893[b]	10.228		6	2	20	11	4	3		4			2		2		4		6												5.49(3), 5.94(3)	30
1899	10.234		34	6	9		20																	6								25
1902	10.236					51		1					2			6															5.53(3), 5.73(3)	30
1917[a]	10.252		31	1	6		4	10			5					1		7		2											5.65(4), 5.92(4)	25
1921	10.256		21		30	6		5		6		5				4	3														5.92(2)	18
1924	10.259		58		11	4	1			10		2		1		1																12
1929	10.263		3		5	7		3		18		19		3	3							9										30
1935	10.269			83														4	2											5.65(1)	10
1940	10.274	3/2	22	13	47			2		1	1	7		1		1		2	1		2	1									2
1942[b]	10.276		3		9	4		7				10	?		5			5												5.57(10)	40
1953	10.286		12	5	3		3						4			16	2													5.98(5)	50
1962	10.295		45	25		1				3		2		1		3															20
1964[b]	10.297		10					8			20		16		7						6									5.57(9), 5.98(4)	20
1973	10.306		9	10		19			11										8											5.62(3)	40
1980	10.313		20	4	3		3		13							5									6					5.73(6)	40
1982	10.315		40	41	1			2				4		2																	10
1986[a]	10.319		72	3																											25

[a] Multiplet [b] Decay corrected for contributions from the next lower resonance
[c] Contribution from the next lower resonance cannot be excluded
[d] In addition a 1 % branch has been observed to the E_x = 6.37 MeV level
[e] In addition 1 % branches have been observed to E_x = 6.32, 6.49, 6.70, 7.08, 7.15, 7.22 and 7.69 MeV
[f] In addition 3 % to E_x = 7.30 MeV
[g] In addition 1 % branches to E_x = 7.08 and 7.15 MeV
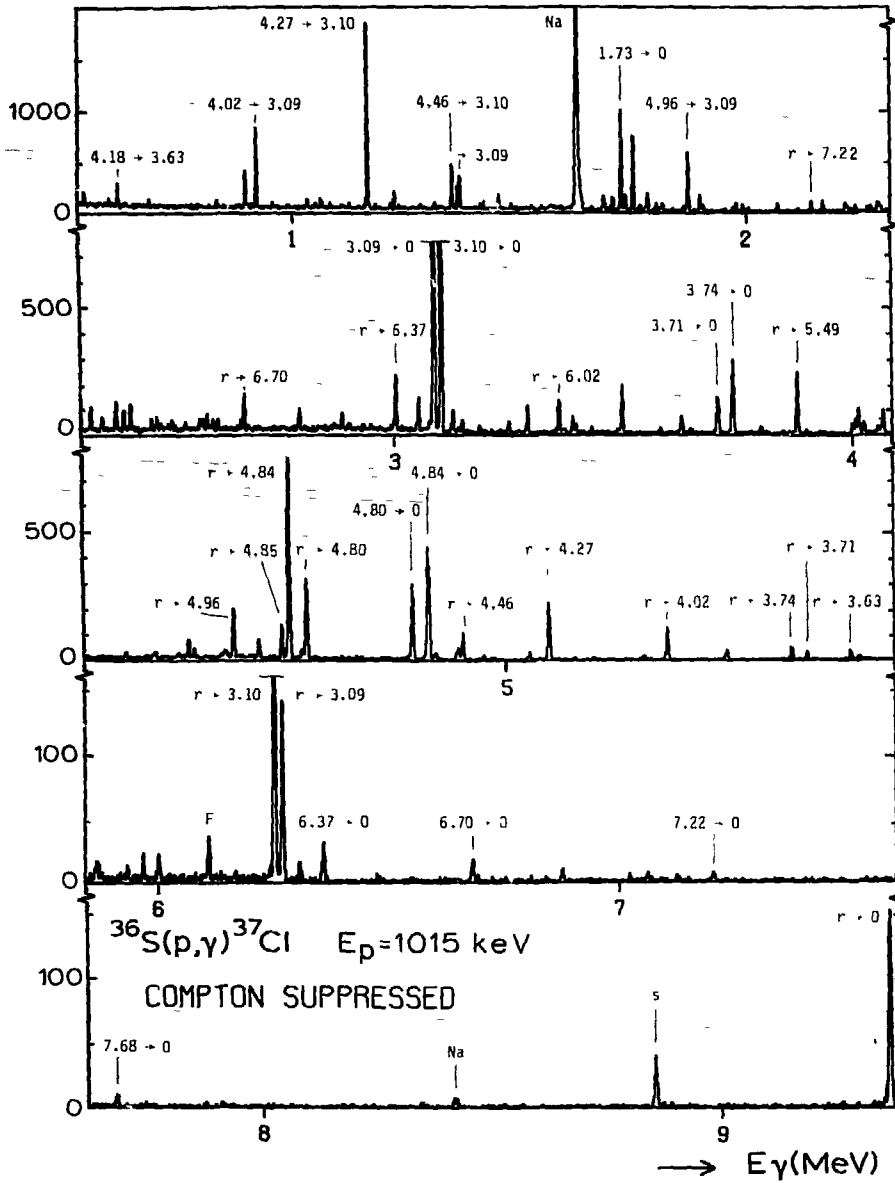[†] For spins and parities, see chapter II

Fig. 7. Compton suppressed γ-ray spectrum of the E_p = 1015 keV
$^{36}S(p,\gamma)^{37}Cl$ resonance, measured at θ = 55° and a solid angle of Ω =
7 msr for a total charge of 5 C. Only selected peaks are labelled.
Peaks marked with s, F and Na are single-escape, room-background,
$^{19}F(p,\alpha\gamma)^{16}O$ and $^{23}Na + p$ peaks, respectively.

4.3. BOUND STATES

In the process of establishing consistent decay schemes for the resonances studied, many hitherto unobserved bound state. have been found.

The criteria for finally adopting a new level, and listing it in table 6, are: (i) the energies of the feeding and decay γ-rays should be consistent within the experimental errors, (ii) the intensity balance of feeding and decay γ-rays should be consistent; unobserved decay was allowed up to 50 %, and (iii) it should have been unambiguously observed in at least two resonances. Because of the rather high ^{34}S content of the target material, the spectra were carefully scanned for ^{35}Cl transitions, especially in the neighbourhood of ^{34}S$(p,\gamma)^{35}$Cl resonances.

In total 30 new bound states were established in this way; they are easily identified in table 6. Apart from a few resolved doublets at lower energies, these new levels mainly fall in the higher excitation range E_x = 5-8 MeV. The group of 18 bound states known from previous experiments but not excited in the present experiment, contains all known high-spin states. It may be expected that most of the other levels in this group also have high angular momenta.

The γ-ray branching ratios of 54 bound states were determined from the θ = 55° spectra. The branchings given in table 7 are averages of the values found at different resonances. For levels at higher excitation energies, of which the feeding is presumably simple, the balance between feeding and decay is used to determine the amount of unknown decay. Upper limits corresponding to two standard deviations for unobserved transitions are given where a useful number could be deduced.

The excitation energies given in table 6 were determined in two steps. First, the energies of the γ-rays deexciting the lower (E_x < 4 MeV) levels were calibrated with the γ-rays from a ^{56}Co source placed

Table 6

Excitation energies (in keV) of bound states of ^{37}Cl

Present work	Literature [a]	Present work	Literature [a]
1 726.58 ± 0.04	1 726.5 ± 0.1	5 528.4 ± 0.6	
3 086.12 ± 0.07	3 086.6 ± 0.4	5 570.1 ± 0.3	5 469.9 ± 0.8
3 103.59 ± 0.08	3 103.3 ± 0.2		5 595 ± 20
3 626.82 ± 0.06	3 626.0 ± 0.5	5 617.9 ± 0.9	
3 707.79 ± 0.09	3 707.9 ± 0.6	5 645.3 ± 0.3	
3 741.05 ± 0.15	3 740.9 ± 0.5		5 708 ± 3
4 011.3 ± 0.6	4 010.6 ± 0.5	5 727.6 ± 0.3	5 725 ± 3
4 016.27 ± 0.09	4 014.8 ± 1.5	5 909.3 ± 0.6	
4 176.64 ± 0.09	4 182 ± 8	5 915.0 ± 0.5	
4 268.87 ± 0.09	4 267.0 ± 1.5		5 931 ± 4
4 272.52 ± 0.17		5 944 ± 2	
4 396.3 ± 0.7	4 393 ± 3	5 978 ± 2	5 960 ± 20
4 459.97 ± 0.15	4 460 ± 3	5 985.9 ± 0.8	
	4 546.2 ± 0.6	6 015.3 ± 0.5	
4 801.21 ± 0.11		6 042.2 ± 0.5	
4 810.9 ± 0.3	4 810.8 ± 0.8		6 050 ± 3
4 837.61 ± 0.10			6 197 ± 3
4 853.96 ± 0.13	4 857 ± 10	6 305.1 ± 0.8	
4 904.2 ± 0.7		6 323.8 ± 0.4	
	4 921 ± 2	6 358 ± 3	6 350 ± 20
	4 932 ± 8	6 372 ± 2	
4 960.8 ± 0.5		6 415 ± 2	
	4 974 ± 3	6 488.3 ± 0.8	
5 009.3 ± 0.8			6 601 ± 5
5 055.2 ± 0.5		6 668.9 ± 0.8	6 670 ± 20
5 059.1 ± 0.7	5 056.0 ± 1.5	6 701.8 ± 0.4	
5 228.7 ± 0.7		6 732 ± 5	
	5 270.7 ± 0.5		7 020 ± 3
	5 283 ± 3	7 079.4 ± 1.2	7 080 ± 20
5 307.4 ± 0.5	5 310 ± 30	7 150 ± 2	
5 317.1 ± 0.7			7 200 ± 4
5 372.5 ± 0.6		7 224.4 ± 0.5	
	5 379 ± 4	7 254.5 ± 1.8	
	5 406 ± 20	7 300 ± 2	7 300 ± 20
5 490.68 ± 0.11	5 500 ± 20	7 686.8 ± 0.5	
	5 547 ± 3		7 735 ± 10

[a] Values adopted in ref.[5], based on the data from several reactions.

Table 7

Branching ratios (in %) of bound states of ^{37}Cl[†]

E_{x1} (MeV)	E_{xf}: J^π :	0 $3/2^+$	1.73 $1/2^+$	3.09 $5/2^+$	3.10 $7/2^-$	3.63 $3/2$	3.71 $3/2^+$	3.74 $5/2^-$	Other levels	Unknown
1.73	$1/2^+$	100								
3.09	$5/2^+$	100	<0.5							
3.10	$7/2^-$	100	<0.1							
3.63	3/2	57 ± 2	43 ± 2	<1	<0.5					
3.71	$3/2^+$	73 ± 3	17 ± 3	10 ± 1	<1					
3.74	$5/2^-$	100	<1	<1	<1					
4.01	$9/2^-$	36 ± 6	<2	<1	64 ± 6	<3				
4.02	$3/2^+$	33 ± 3	19 ± 2	48 ± 3	<1	<1	<1	<1		
4.18	3/2	42 ± 2	<4	21 ± 2	9 ± 2	26 ± 2	<2	2 ± 1		
4.269	(1/2)	<3	100	<1	<1	<2	<2	<1		
4.273	$7/2^-$	<2	<2	3 ± 1	95 ± 1	<1	<1	2 ± 1		
4.40	(5/2)	98 ± 1	<3	<2	<2	<2	<2	2 ± 1		
4.46	$7/2^-$	<4	<4	43 ± 1	57 ± 1	<1	<1	<1		
4.80	$5/2^+$	100	<2	<1	<2	<2	<2	<2		
4.81	(7/2)	<10	<1	<1	68 ± 2	<1	<1	18 ± 3	14 ± 3 → 4.273	
4.84	5/2	72 ± 4	<1	23 ± 3	5 ± 2	<1	<1	<1		
4.85	$5/2^+$	23 ± 6	32 ± 9	17 ± 2	<5	20 ± 2	<3	8 ± 1		
4.90		80 ± 7	<8	20 ± 7	<4	<3	<3	<3		
4.96	3/2	15 ± 5	<5	85 ± 5	<3	<2	<2	<4		
5.01		100	<5	<3	<3	<2	<2	<2		
5.05		70 ± 8	30 ± 8	<10	<5	<10	<3	<3		
5.06		55 ± 8	<5	20 ± 5	15 ± 5	10 ± 5	<5	<5		
5.23		90 ± 3	<7	<4	<4	10 ± 3	<4	<4		
5.31		25 ± 7	25 ± 7	50 ± 10	<10	<10	<10	<10		
5.32		25 ± 7	<3	45 ± 10	<3	<4	<2	30 ± 7		
5.37		<15	40 ± 5	<6	<6	<6	<8	40 ± 5		20
5.49	$5/2^+$	15 ± 5	<5	20 ± 5	20 ± 5	<10	30 ± 9	<5		15
5.53		<5	<15	<10	<10	<10	<20	<10	80 ± 10 → 4.01	20
5.57		<2	<6	7 ± 2	75 ± 2	<2	<2	9 ± 2	9 ± 2 → 4.46	
5.62		88 ± 5	<5	<4	<4	<4	<4	12 ± 5		
5.65		<10	<8	70 ± 10	<15	<5	15 ± 5	<6		15
5.73		<8	<5	<5	<5	<5	<4	60 ± 5	10 ± 5 → 4.01	30
5.91				60 ± 10	40 ± 10					
5.92		60 ± 5	30 ± 5					10 ± 5		
5.94		70 ± 10								30
5.98		60 ± 10		20 ± 10		20 ± 10				
5.99		15 ± 5		40 ± 7			25 ± 5			20
6.02		20 ± 5		8 ± 3		35 ± 5		25 ± 5		12
6.04		30 ± 10				70 ± 10				
6.31		70 ± 10	20 ± 10							10
6.32		35 ± 5		<15				35 ± 5		30
6.36				30 ± 10		30 ± 10				40
6.37		70 ± 5								30
6.42						40 ± 10	25 ± 10		35 ± 10 → 4.269	
6.49		70 ± 20								30
6.67		75 ± 10								25
6.70	5/2	30 ± 5							40 ± 5 → 4.46	30
6.73		70 ± 10								30
7.08		100								
7.15		70 ± 10								30
7.22		55 ± 15	30 ± 15							15
7.25		80 ± 10								20
7.30		60 ± 10	20 ± 10							20
7.69		60 ± 10								40

[†] For spins and parities, see chapter II.

close to the target spot, in the same way as described in sect. 3.5.
The IUPAP-recommended energies [19] for ^{56}Co were used. Subsequently
these energies were used for the calibration of the $\theta = 90^{\circ}$ spectra.
The excitation energies calculated from the γ-ray energies thus obtain-
ed and listed in table 6, are all weighted averages over several reso-
nances. They are compared with the energies listed in the review of
Endt and Van der Leun [5], which are averages of the data from many
different reactions. The present uncertainties are in general conside-
rably smaller than those in the previously reported values. Levels de-
duced from different reactions are considered to be identical if (i)
the energies are equal within the errors and (ii) the decay modes are
at least not contradictory.

5. Summary and discussion

The present experiment yields much new information about resonance
levels and bound states of ^{37}Cl. The main results are summarized in
tables 2-7. The proton capture reaction once again proves to be a pro-
lific source of spectroscopic information, especially when executed
with the presently available high-resolution proton beams and _ditto_
Ge(Li) detectors. In the present experiment the quality of the data
also relies heavily on: the high (81 %) enrichment of the ^{36}S target
material, the preparation of clean targets on clean backings, a clean
vacuum system and the especially designed calibration experiments for
the resonance energies, the resonance strengths and the γ-ray energies.
One of the purposes of the experiments described here, was to ob-
tain the information required for the selection of resonances for the

angular distribution and lifetime measurements to be discussed in the next chapter. At this place the discussion will therefore be limited to the aspects that directly influence the spin and parity assignments.

Resonances. The resonances at E_p = 1079, 1120, 1146, 1196 and 1887 keV at which Hyder and Harris [1,3] measured angular distributions and correlations and Piiparinen et al. [2] studied decay schemes, are shown to be multiplets, see table 2 and fig. 4. The conclusions drawn from those measurements should therefore be considered with caution.

The resonance at E_p = 1887 keV was the subject of a special study by Harris et al. [3] and Keinonen et al. [4]. In fig. 2 it can easily be seen that this resonance is a member of a multiplet. The discrepancies concerning the strength [ref. [1] vs. ref. [3]] and decay [ref. [2] vs. this work] can be ascribed to this multiplet character. The simple decay of this analog (T = 5/2) resonance makes it nevertheless possible to determine its strength, if one chooses the right transition. The yield of the 3.10 → 0 transition shows only one resonance in the energy range of fig. 2. This explains that ref. [3] and the present work agree as to the strength of this resonance.

The 3.71 MeV level. The J^π = 5/2⁻ assignment to this level given by Endt and Van der Leun [5], was based on the combined evidence of $^{34}S(\alpha,p\gamma)^{37}Cl$ work which yields J^π = (3/2⁺,5/2⁻) and the observation [2] of the r → 3.71 MeV transition in the decay of the J^π = 7/2⁻ $^{36}S(p,\gamma)^{37}Cl$ resonance at E_p = 1887 keV, which would imply $J^\pi \neq$ 3/2⁺. This r → 3.71 MeV transition, however, does not occur at the J^π = 7/2⁻ resonance, but at one of the other members of the multiplet, the E_p = 1885 keV resonance. The presently observed 3.71 → 1.73 MeV branch of 17 ± 3 %, combined with the known [5] lifetime of τ_m < 25 fs, would have an M2 strength of >700 W.u. for J^π(3.71) = 5/2⁻. Since the RUL for M2

strengths in the s-d shell is 3 W.u. [14], one concludes to $J^\pi \neq 5/2$.
Combined with the evidence from the $^{34}S(\alpha,p\gamma)^{37}Cl$ reaction quoted above,
this leads to the conclusion $J^\pi(3.71) = 3/2^+$.

The 4.02 MeV level. The lifetime of $\tau_m = 140 \pm 50$ fs (see next chap-
ter) combined with the 19 ± 2 % decay to the $J^\pi = 1/2^+$, 1.73 MeV level
implies $J^\pi \leqslant 5/2^+$. Similarly the application of the RUL for M2 to the
branch to the $J^\pi = 5/2^+$, 3.09 MeV level gives $J^\pi \geqslant 3/2^+$. Conclusion:
$J^\pi = (3/2,5/2)^+$, in agreement with the $l = 2$ assignment from ref.[20].

The 4.27 MeV doublet. A level at $E_x = 4267.0 \pm 1.5$ keV, decaying ex-
clusively to the 1.73-MeV level was reported by Piiparinen et al.[2], a
level at 4270 ± 3 keV, decaying to the 1.73 and 3.09 MeV levels by No-
lan et al.[21], and in $^{38}Ar(d,\tau)^{37}Cl$ a level at $E_x = 4250 \pm 20$ keV was
found with $l = 2$ [ref.[20]]. The present experiment definitely yields
two levels: one with $E_x = 4268.87 \pm 0.09$ keV decaying to the 1.73 MeV
level and a level with $E_x = 4272.52 \pm 0.17$ keV decaying mainly to the
3.10 MeV level. The branch to the 3.09 MeV level has an intensity of
only 3 ± 1 %. As the resolution of the other experiments is too low to
separate the two levels (except probably in that of Piiparinen et al.),
all previous conclusions about spins and parities of the 4.27 MeV
levels should be considered with suspicion.

The 4.46 MeV level. The present observation of a 43 % branch to the
$J^\pi = 5/2^+$, 3.09 MeV level sheds some doubt on the $J = 9/2$ assignment
by Nolan et al.[21]. This branching ratio, combined with the lifetime
$\tau_m = 60 \pm 45$ fs [ref.[21]], implies an E2 strength of 160 ± 120 W.u.,
suggesting that either the J-assignment is incorrect or the lifetime
is longer than 60 fs.

The 4.80/4.81 MeV doublet. The review of ^{37}Cl levels in ref.[5] lists
one level at $E_x = 4.81$ MeV, whereas the present experiments lead to a

4.80/4.81 MeV doublet. On the basis of the decay properties, it is likely that Nolan et al.[21] excited the 4.80 MeV level, Harris et al.[3] and Avrigeanu et al.[22] the 4.81 MeV level, and Piiparinen et al.[2] a mixture of the two. The $J^\pi = 5/2^+$ assignment to the 4.81 MeV level, given in ref.[5] should be disregarded since the doublet was not resolved in the $^{38}Ar(d,\tau)^{37}Cl$ reaction [20], which plays a crucial role in the $J^\pi = 5/2^+$ assignment.

The evaluation [5] of all the previously measured data on ^{37}Cl indicates that unique spin-values could be assigned to ten excited states of this nucleus. Eight of these have been observed in the present experiment. On the basis of the decay studies presented in this chapter, it has been shown that four of these are erroneous or not valid. The next chapter presents angular distribution and lifetime measurements that lead to new spin assignments to these four and many other levels.

REFERENCES

1. A.K. Hyder, G.I. Harris, J.J. Perrizo and F.R. Kendziorski, Phys. Rev. 169 (1968) 899

2. M. Piiparinen, M. Viitasalo and A. Anttila, Physica Scripta 8 (1973) 236

3. G.I. Harris and J.J. Perrizo, Phys. Rev. C2 (1970) 1347

4. J. Keinonen, M. Riihonen and A. Anttila, Physica Scripta 12 (1975) 280

5. P.M. Endt and C. van der Leun, Nucl. Phys. A310 (1978) 1

6. J.W. Maas, E. Somorjai, H.D. Graber, C.A. van den Wijngaart, C. van der Leun and P.M. Endt, Nucl. Phys. A301 (1978) 213

7. W.A. Sterrenburg, G. van Middelkoop, J.A.G. De Raedt,
   A. Holthuizen and A.J. Rutten, Nucl. Phys. A306 (1978) 157

8. M.M. Aléonard, Ph. Hubert, L. Sarger and P. Mennrath, Nucl. Phys.
   A257 (1976) 490

9. Ph. Hubert, M.M. Aléonard, D. Castera, F. Leccia and P. Mennrath,
   Nucl. Phys. A195 (1972) 485

10. M.A. Meyer, I. Venter, W.F. Coetzee and D. Reitmann, Nucl. Phys.
    A264 (1976) 13

11. M.M. Aléonard, C. Boursiquot, Ph. Hubert and P. Mennrath,
    Phys. Lett. 49B (1974) 40

12. B.M. Paine and D.G. Sargood, Nucl. Phys. A331 (1979) 389

13. R.J. Sparks, Nucl. Phys. A265 (1976) 416

14. P.M. Endt, Atomic Data and Nuclear Data Tables 23 (1979) 3

15. P.F.A. Alkemade, C. Alderliesten, C. van der Leun and P. de Wit,
    Nucl. Instr. (to be published)

16. R.G. Helmer, R.J. Gehrke and R.C. Greenwood, Nucl. Instr.
    123 (1975) 51

17. C. Alderliesten and J.A. van Nie, to be published

18. A.H. Wapstra and K. Bos, Atomic Data and Nuclear Data Tables 19
    (1977) 215

19. C. van der Leun, R.G. Helmer and P.H.M. Van Assche, in Atomic
    Masses and Fundamental Constants 6 (1980), eds. J.A. Nolen and
    W. Benenson, Plenum (New York) p. 502

20. P. Doll, H. Mackh, G. Mairle and G.J. Wagner, Nucl. Phys.
    A230 (1974) 329

21. P.J. Nolan, A.J. Brown, P.A. Butler, L.L. Green, A.N. James,
    J.R. Leslie, C.J. Lister, J.D. MacArthur and J.F. Sharpey-Schafer,
    J. of Phys. G2 (1976) 569

22. V. Avrigeanu, D. Bucurescu, E. Drăgulescu, M. Ivaşcu and
    D. Popescu, Rev. Roum. Phys. 20 (1975) 959

23. A.W. Borgi and O. Lönsjö, Nucl. Instr. 17 (1962) 31

24. W. Bruynesteyn, Thesis (1971) Utrecht University

25. H.E. Gove , in Nuclear Reactions I, eds. P.M. Endt and M. Demeur,
    North-Holland (Amsterdam) 1959, p. 259

26. R.J. Elsenaar, Thesis Utrecht University (to be published)

CHAPTER 2

THE REACTION $^{36}S(p,\gamma)^{37}Cl$

(II) Lifetimes, spins and parities of ^{37}Cl levels

Abstract: Analysis of the γ-ray angular distributions measured at nine $^{36}S(p,\gamma)^{37}Cl$ resonances yields the spins and/or parities of 13 bound states of ^{37}Cl in addition to the resonance spins. Among the latter are two $J = 1/2$ resonances. For several other bound states the possible spins have been restricted. Multipolarity mixing ratios have been deduced from the same data. Together with the lifetimes (or lifetime limits) of 25 bound states deduced from DSA measurements, they provide the information required for the application of the RUL's.

Comparison of the experimental information on the ^{37}Cl level scheme with shell-model calculations indicates the configuration of several levels.

1. Introduction

Our knowledge about spins, parities and lifetimes of bound states of ^{37}Cl is mainly due to studies of the $^{34}S(\alpha,p\gamma)^{37}Cl$ reaction [1]. Earlier work on angular distributions at resonances in the reaction $^{36}S(p,\gamma)^{37}Cl$ [ref.[2]] also yielded some information, but was hindered by the low enrichment of the target material and the availability of only NaI detectors. Moreover, several of the resonances studied were shown in ref.[3] to be members of multiplets, which makes the spin assignments ambiguous.

In the present work, angular distribution and Doppler-shift attenuation measurements are performed at nine well-isolated resonances. These measurements yield spins and spin restrictions. Combined with the Recommended Upper Limits (RUL's) for transition strengths [4], they lead to unique spin and/or parity assignments for 13 bound states.

In ref.[3] it was concluded that several previous presumably unambiguous spin assignments to bound states of ^{37}Cl are either incorrect or ambiguous. Because of this, we limited the use of results from previous work to the utmost minimum. In the analysis we only used the values $J^\pi = 3/2^+$, $1/2^+$ and $7/2^-$ for the ^{37}Cl levels at $E_x = 0$, 1.73 and 3.10 MeV, respectively, and the positive parity of the 3.09 MeV level, which seem to be very well founded [1].

2. Experimental method

2.1. GENERAL

The experimental set-up described in ref.[3] has also been used in the present experiments. In order to reduce the measuring time, however, considerably higher beam currents were used, up to 120 µA on target. At low voltage this was possible by the use of a sliding shorting rod. The targets were made as described earlier [3] except that in some experiments at low proton energy copper backings were used.

The high power densities involved (over 20 MW/m^2) necessitated optimum target cooling to obtain a reasonable target lifetime. In the target holder used (see fig. 1) the cooling of the backing at the target spot is achieved by a highly turbulent (Re > 15000) flow of water. The turbulent flow prevents the forming of an insulating vapor layer on the backing that would drastically lower the heat transfer from the backing to the cooling water. With this device the lifetime of the targets was improved by at least a factor of two, compared to the previous construction in which the Reynolds' number of the water flow behind the backing is at least an order of magnitude smaller. At E_p = 1 MeV the yield of a target of 20 µg/cm^2 Ag_2S on Ta decreases to 50 % after 24 hours at 120 µA.

Two out of three Ge(Li) detectors of 80, 95 and 100 cm^3 were used at a distance of 7-10 cm from the target spot, resulting in solid angles of 0.2 - 0.4 sr. During the measurements at E_p > 1.8 MeV the detectors were shielded with 5 mm of Pb to attenuate the low-energy background radiation from the backing.

The measurements were divided in runs of approximately two hours in order to have the measurements at all angles equally affected by drift

and target deterioration. Each run consisted of a sequence of five

angles ($\theta = 0^0$, 30^0, 60^0, 90^0, 45^0) for the angular distributions or

three angles ($\theta = 0^0$, 90^0, 130^0) for the DSA measurements. The spectra

of corresponding angles of different runs were added before the peaks

were analysed. When necessary, corrections were made for gain and base-

line drift in the following way. For each spectrum the position of a

strong low-energy line and a strong high-energy line were compared

with the corresponding peaks in a reference spectrum. The spectrum was

shifted and/or its dispersion changed in order to obtain overlap with
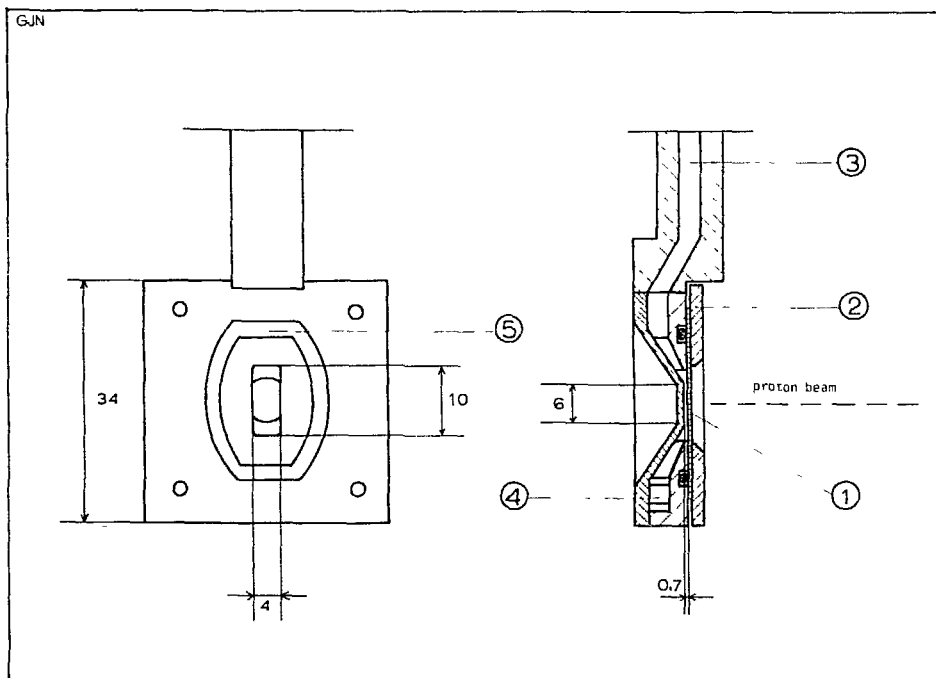
Fig. 1. Target holder for high-power beams. Note the small size ($2.8\ mm^2$) of the water channel directly behind the beamspot.

1. Target on a $2 \times 3\ cm^2$ Cu or Ta backing (thickness 0.3 mm).
2. Ta plate to hold target and O-ring.
3. Exit for cooling water ($25\ cm^3/s$).
4. Entrance for cooling water.
5. Groove for O-ring.

the two peaks in the reference spectrum.

The measurements were controlled by means of home-made electronics, via CAMAC coupled to a PDP 11/34 computer. A BASIC-type program takes care of the whole measuring sequence: (i) positioning of the detectors, (ii) accumulation of the spectra for a preset charge on the target, (iii) writing of spectra on magnetic tape and (iv) calculation of some on-line results. During steps (i), (iii) and (iv) the beam is swept off target by means of bending magnets to conserve the target.

2.2. ANGULAR DISTRIBUTIONS

The almost ever present isotropic decay line of the $J^{\pi} = 1/2^{+}$ level at $E_x = 1.73$ MeV is used as an internal monitor. By normalizing on the area of this line, one essentially also corrects for the eccentricity such that no separate eccentricity measurements are necessary. Strictly speaking, this is only true if the transition of interest has the same γ-ray energy as the monitor line. If the energies are different, two effects have to be considered: (i) γ-rays of different energies are detected in different places in the detector (as is reflected in the energy dependence of the solid angle attenuation factors), (ii) the absorption in the targetholder etc. is different. In our set-up, effect (i) results in an anisotropy of less than 1 % for an eccentricity of 5 %. The influence of effect (ii) is minimized by a non-conventional set-up. Conventionally the target angle is fixed with respect to the proton beam direction, but in our experiments the angle between target and moving detector is fixed, thus keeping the absorption constant.

The relatively high energy of the monitor line is an advantage, as most transitions of interest have energies for which the absorption is roughly the same as for the monitor line.

40

The peak areas obtained from the spectra of each of the two detectors are normalized to the area of the 1.73 MeV peak, tested for mutual consistency and then taken together as one set of data for further analysis.

Because of the spin $J = 0$ of the ^{36}S target nucleus the analysis of the angular distributions is relatively simple. Spins hypotheses were tested by calculating the quantity $\chi^2 = 1/N \times \Sigma \omega_i [I(\theta_i) - W(\theta_i)]^2$ where ω_i is the weight of each measurement, $I(\theta)$ is the measured distribution, $W(\theta) = a_0 [1 + A_2 Q_2 P_2(\cos \theta) + ...]$ is the calculated distribution function corrected for the solid angle damping factors Q, and N is the number of degrees of freedom. In the analysis a_0 is fitted to the data, A_2 and A_4 being calculated for each assumed spin sequence as a function of the mixing ratio. For each spin sequence, χ^2 is thus obtained as a function of δ. Spins were accepted if their χ^2 was less than the value corresponding to the 0.1 % probability limit, irrespective of the corresponding δ value, i.e. no *a priori* assumption was made about "impossible" mixing ratios. For δ the sign convention of Rose and Brink [5] is used. The errors in δ are calculated along the lines indicated by James et al.[6].

2.3. DSA MEASUREMENTS

In angular distribution measurements the target thickness is always a compromise between yield and resolution, especially at higher proton energies where the resonance density is high. As a consequence, long lifetimes cannot be deduced as a by-product from these angular distribution measurements. For the measurement of lifetimes longer than $\tau_m \approx 100$ fs separate experiments were performed, optimized for the Doppler shift measurements, implying (i) a wider angular range of $\theta = 0^\circ - 130^\circ$ instead of $\theta = 0^\circ - 90^\circ$, (ii) simultaneous counting of

a radio-active source to monitor amplifier drifts, and (iii) optimum target thickness in order to ensure that all recoiling atoms are stopped in the target material. To reduce the measuring time, two detectors were used positioned on both sides of the beampipe at three angles $\theta = 0°$, +90° and +130° and $\theta = 0°$, -90° and -130°.

The data were analyzed by fitting the peak positions (obtained from the centre of gravity of the peaks and corrected for electronic drift) with a cos θ function. The resulting Doppler shift was normalized upon the full kinematic shift to obtain F, the fraction of the full shift. The F(τ) curves, of which fig. 2 shows an example, were calculated with the theory of Blaugrund [7].

It is known (see e.g. ref.[8]) that the actual target composition may
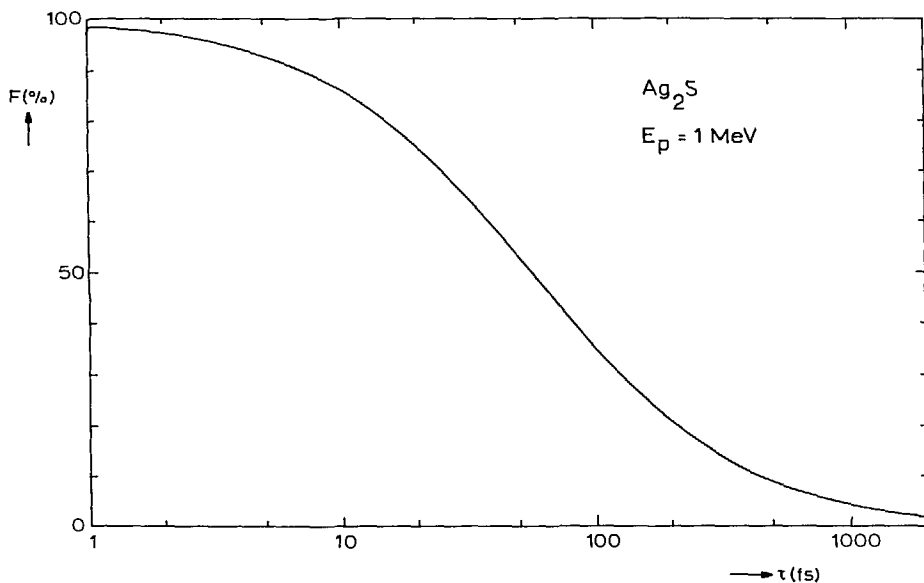
Fig. 2. The Doppler shift F, expressed in percents of the full shift, as a function of the mean life, computed with the theory developed in ref.[7].

differ from the composition of the bulk material. Moreover, the compo-
sition changes during proton bombardment. With Particle Induced X-ray
Excitation (PIXE) we observed differences in the Ag to S ratio of up to
a factor of two between used en unused targets, indicating a depletion
of the sulphur during the bombardment. We estimated the effect of a
changing target composition on the deduced lifetimes by calculating
$F(\tau)$ curves for Ag_nS with n = 1, 2 and 3. For a Doppler shift of F = 50 %
this variation of n causes variations in the lifetimes of up to 20 %.
An extra error of 20 % for this effect was therefore included in the
experimental error. Another 20 % error was added for the uncertainty
in the stopping power. Lifetimes were deduced only at resonances where
the indirect feeding of the level (*viz.* from other states than the reso-
nance) amounted to less than 10 % of the direct feeding. Moreover,
this indirect feeding should proceed via only one level of which the
lifetime should be known. In case of indirect feeding the measured
F-value was of course corrected for the influence of the lifetime of
the intermediate level.

3. Lifetimes

Table 1 shows the measured Doppler shifts F and the resulting lifetimes
τ_m of 25 levels. In some cases only an upper or lower limit could be given,
corresponding to one standard deviation below or above the measured value.
The adopted lifetimes given in the review by Endt and Van der Leun [1]
are tabulated in column 6, except for those levels which on the basis
of the present work are known to be doublets. Where comparison is possible,
one finds no serious discrepancies.

Table 1

Lifetimes of ^{37}Cl levels

E_x (MeV)	E_p (keV)	$F(\tau)$ [a] %	τ_m [b] (fs)	τ_m(fs) This work [c]	Literature [d]
3.09	1 940	70 ± 1	35 ± 1	35 ± 12	45 ± 15
3.10	1 015	<4	>1 000	> 800	22 000 ± 3 000
3.63	1 105	51 ± 1	50 ± 5 [e]	50 ± 20	40 ± 20
3.71	1 015	53 ± 4	50 ± 8 [e]	50 ± 20	<25
3.74	1 015	65 ± 2	30 ± 3	30 ± 10	<20
4.02	1 015	25 ± 8	130 ± $^{130}_{30}$	} 140 ± 50	
	1 872	34 ± 2	145 ± 17		
4.18	1 872	2 ± 10	>400	>300	
4.269	852	27 ± 8	130 ± 60		
	1 219	56 ± 7	48 ± 12	} 60 ± 20	
	1 940	56 ± 3	63 ± 8		
4.273	1 015	33 ± 3	107 ± 12	110 ± 40	
4.40	699	74 ± 5	17 ± 5	} 19 ± 7	
	1 872	76 ± 8	27 ± 12		
4.46	1 015	37 ± 5	90 ± 15	} 90 ± 30	60 ± 45
	1 105	33 ± 9	110 ± 50		
4.80	1 015	>90	<8	<10	
4.81	1 015	48 ± 4	60 ± 9	60 ± 20	
4.84	1 015	91 ± 3	6 ± 2	6 ± 3	
4.85	699	>97	<4	<5	
4.96	1 105	76 ± 7	20 ± 7	20 ± 9	
5.01	1 940	93 ± 4	7 ± 4	7 ± 4	
5.23	1 219	>90	<8	<10	
5.49	1 015	73 ± 3	22 ± 4	22 ± 8	
5.65	1 872	>90	<10	<12	
6.02	1 219	88 ± 8	9 ± 7	9 ± 7	
6.04	1 219	78 ± 10	20 ± 10	20 ± 12	
6.70	1 015	>95	<4	<5	
7.22	1 015	>90	<8	<10	
7.69	1 015	76 ± 5	19 ± 5	19 ± 7	

[a] Averaged over different decay branches, where applicable.

[b] Statistical errors only.

[c] Average values; 20 % systematic errors have been added to the statistical error both for the uncertainty in the target composition and for the uncertainty in the stopping power.

[d] Values adopted in ref.[1] on the basis of all the previously available data.

[e] Corrected for indirect feeding.

The lifetimes of the bound states are used in combination with their branching ratios [3] to calculate transition strengths. Application of the RUL's then restricts the possible J^π values. Only those J^π values were considered in the angular distribution analysis.

4. Spins and parities

4.1. RESONANCES

For the purpose of a concise presentation of the data, the measured angular distributions were fitted with $W(\theta) = a_0[1 + A_2P_2(\cos \theta) + A_4P_4(\cos \theta)]$. Table 2 lists the coefficients A_2 and A_4 for all the primary transitions analyzed. In case the value of A_4 was less than twice its error, the angular distribution was fitted with an A_2 only.

The two last columns of this table present the deduced mixing ratios δ for the primary transitions to states with known spin. Mixing ratios which are allowed on the basis of the angular distributions, but which do result in a violation of the RUL's, have been omitted. When more than two δ-values are possible, no value is quoted.

The spins of the resonances studied are listed in table 3. Column 2 presents the spins and parities compatible with the RUL's applied to the strengths of the branches to the ground state ($J^\pi = 3/2^+$), the 1.73 MeV level ($J^\pi = 1/2^+$) and the 3.10 MeV level ($J^\pi = 7/2^-$), as given in ref.[3]. Column 3 gives the spins that could not be rejected at a 99.9 % confidence level on the basis of the analysis of the angular distributions. The adopted resonance spins are tabulated in column 4. Plots of normalized x^2 values resulting in unique assignments of resonance spins are shown in figs. 3a - 3c.

Table 2

Angular distribution coefficients and mixing ratios of primary $^{36}S(p,\gamma)^{37}Cl$ transitions

E_p (keV)	$E_{x1} \to E_{xf}$ (MeV)	100 A_2	100 A_4	δ_1	δ_2
678	9.05 → 0	52 ± 5		-0.08 ± 0.02	-2.87 ± 0.17
	→ 3.63	68 ± 9		-0.23 ± 0.05	-2 0 ± 0.2
	→ 3.71	35 ± 10		0.02 ± 0.07	-4.3 ± 1.4
	→ 4.18	39 ± 3		-0.00 ± 0.02	-3.8 ± 0.3
699	9.07 → 0	44 ± 1		-0.042 ± 0.008	-3.3 ± 0.1
	→ 3.09	-12 ± 2		-0.02 ± 0.02	5.2 ± 0.5
	→ 4.02	38 ± 7		-0.00 ± 0.05	-3.9 ± 0.8
	→ 4.40[a]	9 ± 4		0.17 ± 0.05	
852	9.22 → 0	38 ± 2		0.005 ± 0.013	-4.0 ± 0.2
	→ 4.269[b]	-43 ± 5		-0.01 ± 0.04	1.8 ± 0 2
	→ 5.37	32 ± 8			
924	9.27 → 0	0 ± 2			
	→ 1.73	3 ± 8			
	→ 3 63	2 ± 4			
	→ 4.02	-1 ± 3			
	→ 6.04	4 ± 6			
1 015	9.37 → 0	-37 ± 2		-0.020 ± 0.006	
	→ 3.09	52 ± 2	-6 ± 2	-0.08 ± 0.03	
	→ 3.10	-17 ± 2		-0.027 ± 0 010	
	→ 3.71	-35 ± 5		0.00 ± 0.02	
	→ 3.74	51 ± 7		-0.07 ± 0.06	
	→ 4.273	-9 ± 3		0.018 ± 0.013	
	→ 4.46	-6 ± 4		0.05 ± 0.02	
	→ 4.80	40 ± 3		0.04 ± 0.02	
	→ 4.81[c]	-3 ± 14		0.08 ± 0 10	
	→ 4.84	43 ± 2		0.011 ± 0.015	
	→ 4.85	43 ± 2		0.015 ± 0 016	
	→ 4 96	-33 ± 3		-0.031 ± 0.012	
	→ 5.49	56 ± 6		-0.13 ± 0.07	-0.95 ± 0.17
	→ 6.02	-36 ± 4			
	→ 6.70	46 ± 5		-0.00 ± 0.04	
	→ 7.22	42 ± 8			
	→ 7.69	34 ± 5			
1 105	9.46 → 3.09	26 ± 7		0.17 ± 0 05	-1 8 ± 0.2
	→ 3.63	-40 ± 1		0 011 ± 0 004	
	→ 4.18	-41 ± 2		0 013 ± 0.009	
	→ 4 40[a]	32 ± 7	-15 ± 6	0 11 ± 0.07	
	→ 4.46	-8 ± 6		0.01 ± 0 05	
	→ 4 96	-73 ± 7		0.19 ± 0 04	
1 219	9.57 → 0	0 ± 1			
	→ 3.71	-0 ± 4			
	→ 4.269[b]	1 ± 2			
	→ 5.23	-10 ± 6			
	→ 6 02	-2 ± 2			
	→ 6.04	-6 ± 5			
1 872	10 21 → 0	48 ± 2		-0 067 ± 0.012	-3.02 ± 0.12
	→ 3 71	37 ± 2		0.009 ± 0.012	-4.0 ± 0.2
	→ 4.02	38 ± 2		0.002 ± 0.011	-3.9 ± 0.2
	→ 4.18	35 ± 5		0.02 ± 0.02	-4.2 ± 0.6
	→ 4.40[a]	-13 ± 10		-0.01 ± 0.09	
	→ 4.96	56 ± 8		-0.13 ± 0.06	-25 ± 0.5
	→ 5.65	33 ± 5			
1 940	10.27 → 0	50 ± 1		-0.081 ± 0.008	-2.89 ± 0.07
	→ 3.09	-8 ± 1		0.016 ± 0 007	
	→ 4.269[b]	-50 ± 2		0.01 ± 0.01	1.70 ± 0.04
	→ 5.01	-50 ± 7			

[a] For J = 5/2   [b] For J = 1/2   [c] For J = 7/2

Table 3

Arguments for spin assignments to
$^{36}S(p,\gamma)^{37}Cl$ resonance levels

E_p (MeV)	J^π		
	decay	ang. distr.	conclusion
678	$1/2 - 7/2^+$	3/2	3/2
699	$1/2 - 5/2^+$	3/2	3/2
852	$1/2 - 5/2$	3/2	3/2
924	$1/2 - 5/2$	1/2, 3/2	$1/2$ [a]
1015	$3/2^- - 7/2^+$	3/2, 5/2	$5/2$ [b]
1105	$1/2 - 7/2^+$	3/2, 5/2	$5/2$ [b]
1219	$1/2 - 7/2^+$	1/2, 3/2	$1/2$ [a]
1872	$1/2 - 5/2^+$	3/2	3/2
1940	$1/2 - 5/2^+$	3/2	3/2

[a] Ref. [9].   [b] See text.

The $E_p = 1015$ keV, $E_x = 9.37$ MeV resonance. Analysis of the r → 3.10 MeV transition leads to $J_r = 3/2, 5/2$ (fig. 3b). A $J_r^\pi = 3/2^+$ assignment would lead to an M2 strength of 80 W.u., whereas the large M3 admixture implied by a $J_r^\pi = 3/2^-$ assignment would have a strength of 40 kW.u., well above the RUL's of 3 and 10 W.u., respectively. Conclusion: $J_r = 5/2$.

The $E_p = 1105$ keV, $E_x = 9.46$ MeV resonance. Analysis of the r → 3.63 MeV transition[†] gives $J_r = 3/2, 5/2$. The r → 4.46 MeV transition[†] leads to $J_r = 3/2, 5/2, 7/2$. A $J^\pi = 3/2^+$ assignment would lead to an M2

[†] The J^π-values of table 5 are used.
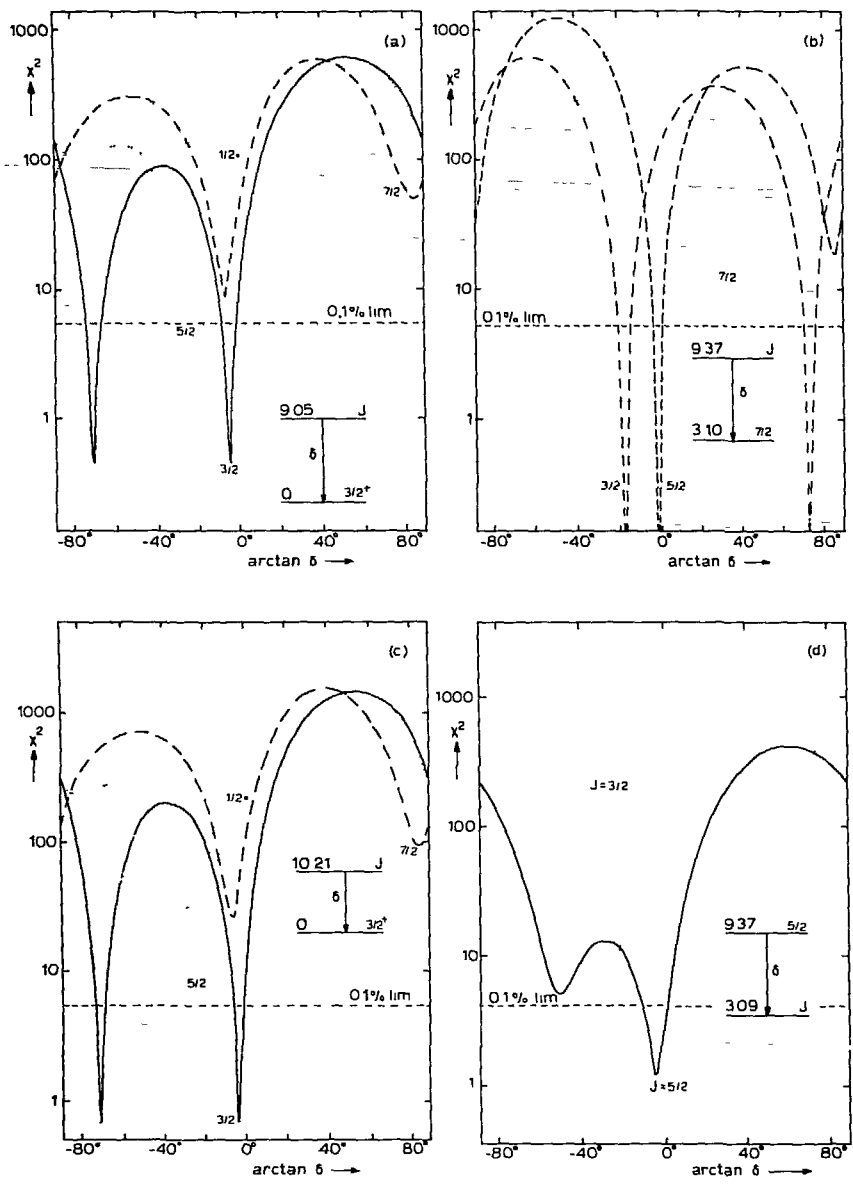
Fig. 3. Plots of χ^2 versus arctan δ for the angular distributions of primary transitions used to obtain spins of resonances and bound states.

a) E_p = 678 keV, E_x = 9.05 MeV resonance.

b) E_p = 1015 keV, E_x = 9.37 MeV resonance.

c) E_p = 1872 keV, E_x = 10.21 MeV resonance.

d) E_p = 1015 keV, E_x = 9.37 MeV resonance; r → 3.09 MeV transition.

strength of 40 W.u., whereas the large M3 admixture implied by a J^π = 3/2⁻ assignment would have a strength of 20 kW.u., well above the RUL's of 3 and 10 W.u., respectively. Conclusion: J_r = 5/2.

The E_p = 678, 699, 1872 and 1940 keV resonances. These resonances with E_x = 9.05, 9.07, 10.21 and 10.27 MeV all have J_r = 3/2, on the basis of the angular distribution of the ground-state transition (figs. 3a and 3c).

The E_p = 924 keV, E_x = 9.29 MeV and E_p = 1219 keV, E_x = 9.57 MeV resonances. The angular distributions of the transitions to the 1.73 MeV level and the ground state for the E_p = 924 keV and E_p = 1219 keV resonances, respectively, give J_r < 5/2. The exclusion of the J_r = 3/2 solution, based on the arguments given in appendix A, leads to unique assignments of J_r = 1/2.

4.2. BOUND STATES

Spins of bound states were determined from the simultaneous analysis of feeding (primary) and decay transitions of the levels of interest. Only in a few cases the analysis of the primary transitions suffices for a unique spin assignment.

Table 4a summarizes the angular distribution data for secondary transitions. The first column shows which transitions have been analyzed. The second and third columns list the energies of the resonances at which the transitions have been studied, and the measured angular distribution coefficients, respectively. The last two columns give the resulting mixing ratios for transitions between bound states. Mixing ratios that would result in a violation of one of the RUL's have been omitted.

Average values for the mixing ratios deduced from the present work

Angular distribution coefficients and mixing ratios

of γ-ray transitions between bound states of ^{37}Cl

$E_{xi} \rightarrow E_{xf}$ (MeV)	E_p (keV)	100 A_2	δ	
3.09 → 0	1 940	53 ± 1	−0.74 ± 0.02 or	−2.7 ± 0.1
3.63 → 0	1 105	33 ± 1	−0.018 ± 0.010	−3.6 ± 0.2
3.63 → 1.73	1 105	−32 ± 1	−0.033 ± 0.010	−3.5 ± 1.1
3.71 → 0	1 015	−19 ± 3	0.45 ± 0.04	5.8 ± 1.1
	1 872	−5 ± 3	0.44 ± 0.15	6 ± $^{12}_{3}$
3.71 → 1.73	1 872	16 ± 3	−0.9 ± $^{0.2}_{0.6}$	−4 ± $^2_6$
3.71 → 3.09	1 872	−6 ± 3	−0.19 ± 0.16	
3.74 → 0	1 015	−22 ± 2	−0.024 ± 0.016	
4.02 → 0	1 872	−6 ± 2	0.49 ± 0.12	5 ± 3
4.02 → 1.73	1 872	−15 ± 3	0.20 ± 0.12	1.1 ± 0.3
4.02 → 3.09	699	4 ± 3	0.3 ± 0.2	2 ± 1
	1 872	1 ± 1	0.15 ± 0.06	2.7 ± 0.5
4.18 → 0	678	9 ± 6	−0.0 ± 0.2	−3 ± $^2_7$
	1 105	26 ± 10	0.1 ± 0.7	−5 ± 3
	1 872	15 ± 7	−0.3 ± 0.2	−1.7 ± $^{0.3}_{2.1}$
4.18 → 3.09	678	0 ± 5	0.1 ± 0.3	3 ± $^7_2$
	1 105	−6 ± 5	0.03 ± 0.05	4.1 ± 0.8
	1 872	−13 ± 7	−0.4 ± 0.3	−5 ± $^2_{16}$
4.18 → 3.10	678	9 ± 10	−0.04 ± 0.12	−3 ± $^1_2$
	1 105	4 ± 13	−0.10 ± 0.16	1.8 ± 0.7
	1 872	− 1 ± 10	−0.0 ± 0.4	2.3 ± 1.6
4.18 → 3.63	678	9 ± 4	−0.04 ± 0.12	−3 ± $^1_2$
	1 105	−1 ± 4	−0.01 ± 0.03	−3.7 ± 0.4
	1 872	11 ± 4	−0.13 ± 0.18	−2.5 ± 1.3
4.269 → 1.73	852	1 ± 7		
	1 940	1 ± 4		
4.273 → 3.10	1 015	35 ± 2	0.06 ± 0.02	
4.40[b] → 0	699	−21 ± 6	−0.04 ± 0.03	4.0 ± 0.5
	1.105	+10 ± 30	−0.3 ± 0.3	
	1 872	−11 ± 6	−0.11 ± 0.04	5.6 ± 1.3

Angular distribution coefficients and mixing ratios
of γ-ray transitions between bound states of ^{37}Cl

$E_{xi} \rightarrow E_{xf}$ (MeV)	E_p (keV)	$-100\,A_2$		δ
4.46 → 3.09	1 015	−21 ± 3	−0.041 ± 0.013	
	1 105	−22 ± 3	−0.04 ± 0.02	
4.46 → 3.10	1 015	31 ± 2[a]	0.14 ± 0.03	−1.27 ± 0.08
	1 105	28 ± 3	0.16 ± 0.04	−1.26 ± 0.10
4.80 → 0	1 015	−53 ± 2	0.236 ± 0.014	
4.81[c] → 3.10	1 015	37 ± 7	0.06 ± 0.09	−1.1 ± 0.2
4.81[c] → 3.74	1 015	−15 ± 11	−0.1 ± 0.7	
4.84 → 0	1 015	20 ± 2	−0.047 ± 0.013	
5.01 → 0	1 940	7 ± 7		
5.49 → 3.09	1 015	−16 ± 6	0.71 ± 0.15	>6
5.49 → 3.71	1 015	−12 ± 8	−0.09 ± 0.05	$6 \pm {}^3_1$
5.65 → 3.09	1 872	−11 ± 5		
6.70 → 0	1 015	−27 ± 10	0.01 ± 0.05	
6.70 → 4.46	1 015	−18 ± 10	−0.09 ± 0.10	
7.22 → 0	1 015	−36 ± 14		
7.69 → 0	1 015	1 ± 13		

[a] And $A_4 = -0.06 \pm 0.03$.
[b] For J(4.40) = 5/2.
[c] For J(4.81) = 7/2.

are presented and compared with the available literature data in table 4b. A discrepancy occurs for the 3.09 → 0 MeV transition, but the quoted uncertainty in the literature value is quite large.

The figs. 4 and 5 show plots of χ^2 values calculated for the spin determinations of some bound states. All χ^2 values are normalized and the corresponding 0.1 % confidence limit is indicated. The calculations

Table 4b

Summary of measured mixing ratios
for transitions between bound states of ^{37}Cl

$E_{xi} \rightarrow E_{xf}$ (MeV)	δ		Literature [b]
	Present work [a]		
3.09 → 0	−0.74 ± 0.02 or	−2.7 ± 0.1	−1.5 ± 0.4
3.63 → 0	−0.018 ± 0.010	−3.6 ± 0.2	
3.63 → 1.73	−0.033 ± 0.010	−3.5 ± 1.1	
3.71 → 0	0.45 ± 0.04	5.8 ± 1.1	
3.71 → 1.73	−0.9 ± $^{0.2}_{0.6}$	−4 ± $^{2}_{6}$	
3.71 → 3.09	−0.19 ± 0.16		
3.74 → 0	−0.024 ± 0.016		−0.07 ± 0.03
4.02 → 0	0.49 ± 0.12	5 ± 3	
4.02 → 1.73	0.20 ± 0.12	1.1 ± 0.3	
4.02 → 3.09	0.16 ± 0.06	2.5 ± 0.5	
4.18 → 0	−0.13 ± 0.14	−2.5 ± 1.2	
4.18 → 3.09	0.03 ± 0.05		
4.18 → 3.10	−0.06 ± 0.10		
4.18 → 3.63	−0.01 ± 0.03		
4.273 → 3.10	0.06 ± 0.02		
4.40 [c] → 0	−0.06 ± 0.03	4.2 ± 0.5	
4.46 → 3.09	−0.041 ± 0.013		
4.46 → 3.10	0.14 ± 0.03	−1.27 ± 0.08	−0.1 ± 0.2
4.80 → 0	0.236 ± 0.014		
4.81 [d] → 3.10	0.06 ± 0.09	−1.1 ± 0.2	
4.81 [d] → 3.74	−0.1 ± 0.7	7 ± 3	
4.84 → 0	−0.047 ± 0.013		
5.49 → 3.09	0.71 ± 0.15		
5.49 → 3.71	−0.09 ± 0.05		
6.70 → 0	0.01 ± 0.05		
6.70 → 4.46	−0.09 ± 0.10		

[a] Average from the values listed in table 4a.

[b] Values adopted in the review given in ref.[1].

[c] For J(4.40) = 5/2.

[d] For J(4.81) = 7/2.

were performed by simultaneously fitting all the relevant transitions. Although only one-dimensional χ^2 plots are given, these cross sections through the χ^2 plane along one minimum δ-value yield the same information as multi-dimensional plots.

Table 5 summarizes the arguments for J^{π} assignments to bound states. Column 3 lists the results from the angular distribution analysis at the different resonances given in column 2. Application of the RUL's on the transition strengths calculated with the δ-values corresponding to each J-hypothesis, leads to the results listed in columns 4 and 5. The other data required for the calculation of these strengths have been taken from section 3 and chapter I. Column 6 summarizes the results of the present work. Comparison with other work, listed in columns 7 and 8, results in the spin and parity assignments tabulated in column 9.

When two possible J^{π} values remain, often one solution is far more likely than the other, i.e. it results in lower χ^2 values and/or smaller primary mixing ratio. The other solution, however, could not be excluded on the basis of "strong arguments" [1]. In these cases we use the notation $J_1(J_2)$, where J_1 is the most probable value. The restriction to the value J_1 or J_2, however, is based on strong arguments. Most of the unambiguous assignments do not require a separate discussion per level. They are clear from the data in table 5 and figs. 4 and 5. For some bound states additional remarks are given below.

The 3.63 MeV level. The angular distribution at the E_p = 678 keV resonance definitely excludes J = 5/2 (fig. 4a). The measured mixing ratio of δ = -0.033 ± 0.010 for the 3.63 → 1.73 MeV transition would lead to an unusually large, but not impossible M2 strength of 1.7 ± 1.2 W.u. if the level would have J^{π} = 3/2⁻.

The 4.18 MeV level. A J = 7/2 assignment is excluded on the basis of the mixing ratio of the primaries at the E_p = 678 and 1872 keV re-
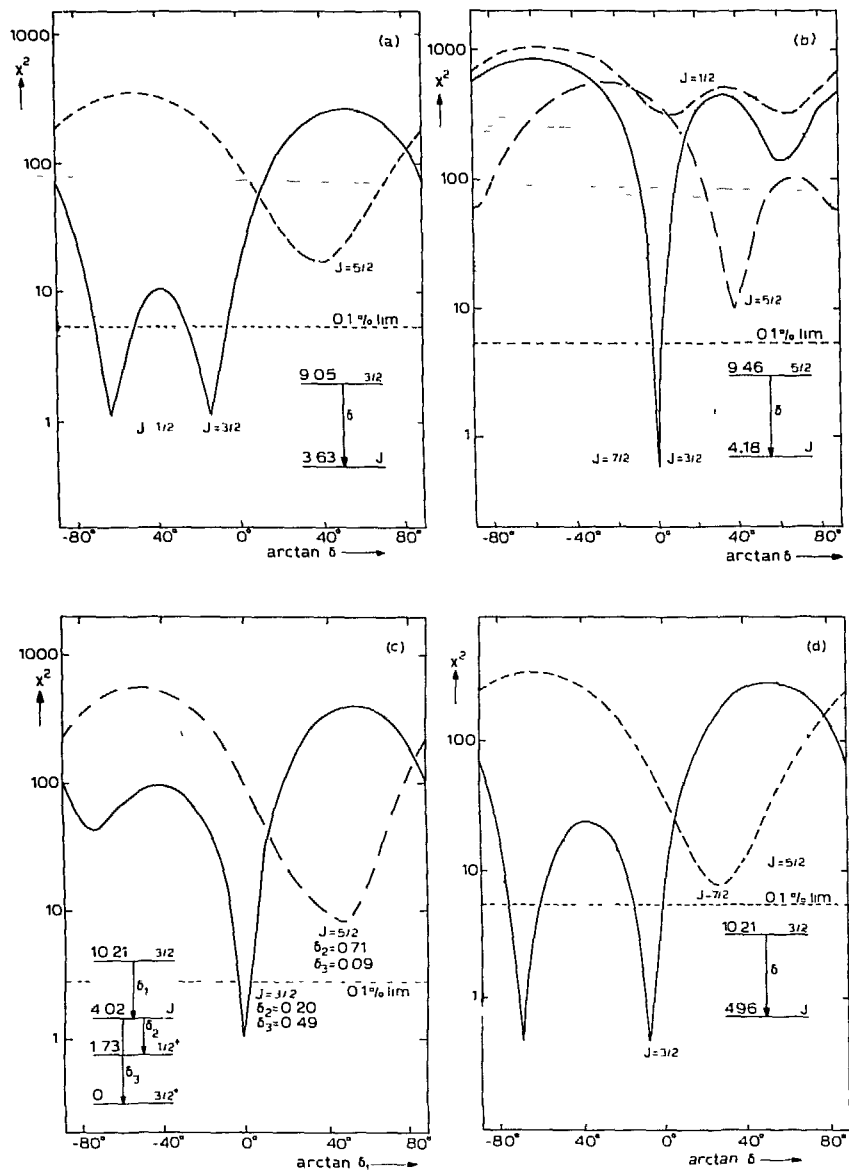
Fig. 4. Plots of χ^2 versus arctan δ for the angular distributions of primary transitions used to obtain spins of bound states.

a) $E_p = 678$ keV, $E_x = 9.05$ MeV resonance; $r \to 3.63$ MeV transition.

b) $E_p = 1105$ keV, $E_x = 9.46$ MeV resonance; $r \to 4.18$ MeV transition.

c) $E_p = 1872$ keV, $E_x = 10.21$ MeV resonance; $r \to 4.02$, $4.02 \to 1.73$ and and $4.02 \to 0$ MeV transitions.

d) $E_p = 1872$ keV, $E_x = 10.21$ MeV resonance; $r \to 4.96$ MeV transition.

Table 5

Arguments for spin and parity assignments to bound states of ^{37}Cl

E_x (MeV)	E_p (keV)	J^π ang. distr.[a]	γ-feeding[b]	γ-decay[c]	this work	$(\alpha,p\gamma)$[d]	(d,τ)[e]	conclusion
3.09	1 015	3/2 - 7/2			}5/2	5/2$^+$	(3/2, 5/2)$^+$	5/2$^+$
	1 105	3/2, 5/2						
	1 940	5/2, 7/2	≠7/2					
3.63	678	1/2, 3/2			}3/2$^{(+)}$ g	3/2,5/2		3/2$^{(+)}$
	1 105	≠1/2 f						
3.71	678	3/2, 5/2		≠5/2$^-$	}3/2$^+$	3/2$^+$, 5/2		3/2$^+$
	1 015	3/2, 5/2						
	1 872	3/2, 5/2		≠3/2$^-$, 5/2				
3.74	659	1/2 - 7/2			}3/2, 5/2	5/2$^-$		5/2$^-$
	1 015	3/2, 5/2						
4.02	699	3/2 - 7/2	≠7/2	≠3/2$^-$, 5/2$^-$	}3/2$^+$		(3/2, 5/2)$^+$	3/2$^+$
	1 872	3/2		≠3/2$^-$				
4.18	678	1/2 - 7/2	≠7/2		}3/2$^{(-)}$ g			3/2$^{(-)}$
	1 105	3/2, 7/2						
	1 872	3/2 - 7/2	≠7/2					
4.269	852	1/2(3/2)			}1/2(3/2)			1/2(3/2)
	1 940	1/2(3/2)						
4.273	1 015	7/2, 9/2		≠7/2$^+$, 9/2	7/2$^-$			7/2$^-$
4.40	699	3/2,5/2			}5/2(3/2)			5/2(3/2)
	1 105	1/2 - 7/2						
	1 872	1/2 - 7/2	≠7/2					
4.46	1 015	5/2, 7/2		≠5/2, 7/2$^+$	7/2$^-$	9/2		7/2$^-$
4.80	1 015	5/2		≠5/2$^-$	5/2$^+$			5/2$^+$
4.81	1 015	3/2 - 9/2	≠9/2	≠3/2, 5/2$^+$	7/2(5/2$^-$)			7/2(5/2$^-$)
4.84	1 015	5/2			5/2			5/2
4.85	1 015	5/2 - 9/2		≠5/2$^-$, 7/2, 9/2	5/2$^+$			5/2$^+$
4.96	1 015	3/2, 7/2			}3/2			3/2
	1 105	3/2, 5/2						
	1 872	3/2						
5.49	1 015	3/2 - 7/2		≠3/2, 5/2$^-$, 7/2	5/2$^+$		(3/2, 5/2)$^+$	5/2$^+$
5.65	1 872	3/2 - 7/2	≠7/2	≠3/2$^-$, 5/2$^-$, 7/2	(3/2, 5/2)$^+$			(3/2, 5/2)$^+$
6.02	1 015	3/2 - 7/2		≠7/2$^-$	}3/2(5/2)			3/2(5/2)
	1 219		≠7/2					
6.70	1 015	3/2, 5/2		≠3/2	5/2			5/2
7.22	1 015	3/2, 5/2		≠3/2$^-$	5/2(3/2$^+$)			5/2(3/2$^+$)

[a] Values not listed are excluded at a 99.9 % confidence level.

[b] From the application of recommended upper limits (RUL, see ref.[4]) to the γ-transitions from the resonance levels mentioned, for resonance branchings and strengths, see tables in chapter I, respectively, the mixing ratios for rejected spin sequences are not listed.

[c] From the RUL's applied to the strengths of the decay γ-rays, as calculated from the branchings given in chapter I, table 7 and the lifetimes presented in table I.

[d] Ref.[10]; ^{34}S$(\alpha,p\gamma)^{37}$Cl at E_d = 9 - 17 MeV.

[e] Ref.[11]; ^{38}Ar$(d,\tau)^{37}$Cl at E_d = 52 MeV.

[f] Anisotropic decay, see table 4a.

[g] See text.
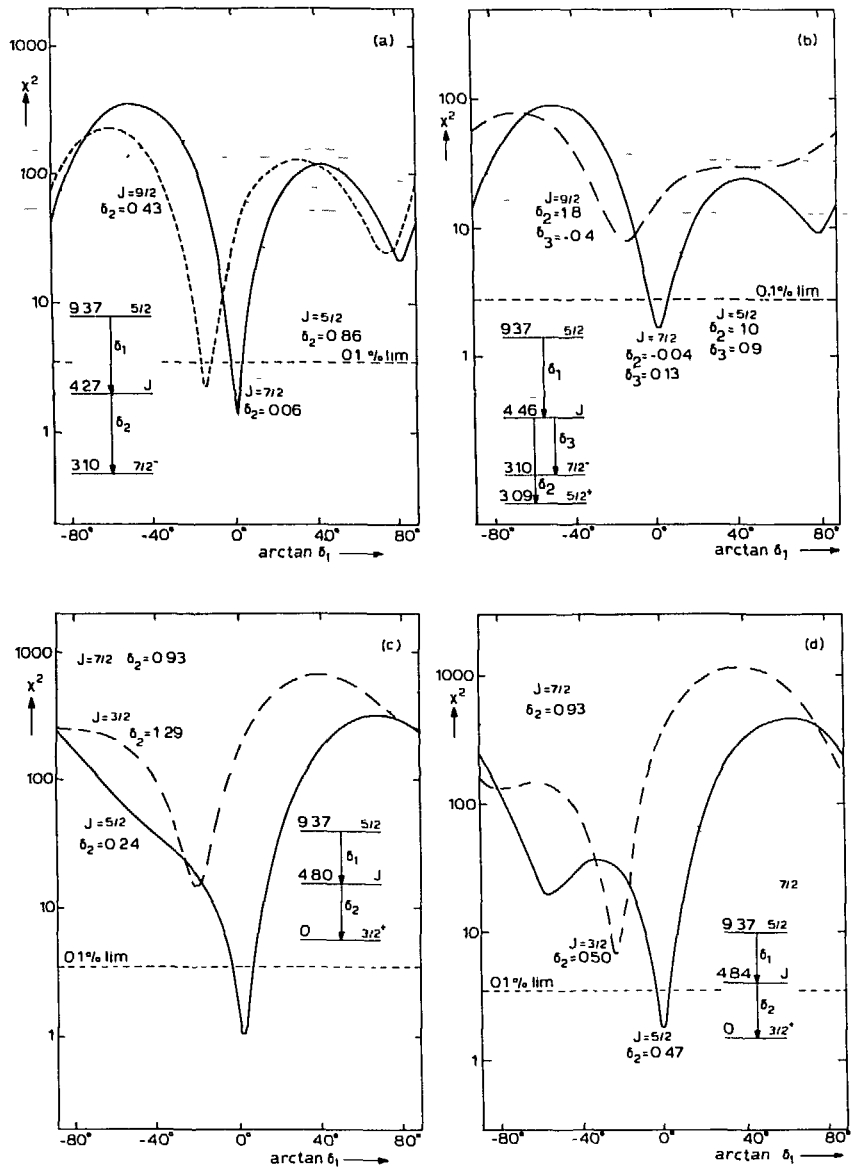
Fig. 5. Plots of χ^2 versus arctan δ for the angular distributions of primary transitions at the $E_p = 1015$ keV, $E_x = 9.37$ MeV resonance, used to obtain spins of bound states.

a) $r \rightarrow 4.273 \rightarrow 3.10$ MeV transitions.

b) $r \rightarrow 4.46$, $4.46 \rightarrow 3.10$ and $4.46 \rightarrow 3.09$ MeV transitions.

c) $r \rightarrow 4.80 \rightarrow 0$ MeV transitions.

d) $r \rightarrow 4.84 \rightarrow 0$ MeV transitions.

sonances, whereas the angular distribution at the E_p = 1105 keV reso-
nance excludes J = 5/2 (fig. 4b). Conclusion: J = 3/2. Because the
lifetime could not be determined (τ_m > 300 fs) only lower limits can
be calculated for the secondary transition strengths. In case a later
lifetime measurement would lead to a value τ_m < 100 ps, which is quite
likely for such a low-spin level, the strength of the transition to
the 3.10 MeV, J^π = 7/2$^-$ level would exclude J^π = 3/2$^+$ and thus lead to
a J^π = 3/2$^-$ assignment.

The 4.02 MeV level. The angular distributions at the E_p = 1872 keV
resonance lead to J = 3/2 (fig. 4c). The large mixing ratio of the
4.02 → 3.09 MeV transition would imply an M2 strength of 500 ± 200 W.u.
for J^π(4.02) = 3/2$^-$. Conclusion: J^π = 3/2$^+$.

The 4.273 MeV level. The angular distributions at the E_p = 1015 keV
resonance lead to J = 7/2 or 9/2 (fig. 5a). The strong octupole ad-
mixture of the primary transition excludes J = 9/2. The quadrupole
admixture of the 4.27 → 3.10 MeV transition would have an M2 strength
of 50 ± 15 W.u. for J^π = 7/2$^+$. Conclusion: J^π = 7/2$^-$.

The 4.40 MeV level. The angular distributions measured at three
resonances indicate a preference for J = 5/2, but the J = 3/2 possi-
bility cannot be excluded. The preference for a J = 5/2 assignment
is illustrated in table 6, which lists the primary mixing ratios δ_1
corresponding to the spins J(4.40) = 3/2 and 5/2, and giving consis-
tent secondary mixing ratios δ_2. The J = 3/2 solution requires strong
quadrupole admixture of the primary transitions at all three resonances,
whereas these transitions are practically pure dipole in the case of
J = 5/2.

The 4.46 MeV level. The angular distributions measured at the
E_p = 1015 keV resonance definitely exclude the previously accepted
value J = 9/2 (fig. 5b), the only acceptable values being J = 5/2

Table 6

Mixing ratios of three r → 4.40 MeV and the 4.40 → 0 MeV
transitions for J(4.40 MeV) = 3/2 and 5/2

J(4.40)	arctan δ_1 (r → 4.40)			arctan δ_2 (4.40 → 0)
E_p(keV):	699	1105	1872	
3/2	-87 ± 2°	-19 ± 2°	86 ± 4°	5 ± 3° or -83 ± 4°
5/2	10 ± 3°	6 ± 4°	-1 ± 5°	3 ± 2° or 78 ± 2°

or 7/2. The mixing ratios of the transition to the E_x = 3.10 MeV,
J^π = 7/2$^-$ level corresponding to J = 5/2 and 7/2, would result in
unacceptable M2 strengths of 1.4 ± 0.5 kW.u. and 70 ± 40 W.u. for
J^π = 5/2$^+$ and 7/2$^+$, respectively. The mixing ratio of the transition
to the E_x = 3.09 MeV, J^π = 5/2$^+$ level excludes J^π = 5/2$^-$,
since it would imply an M2 strength of 1.0 ± 0.3 kW.u. For J^π = 7/2
this transition has δ = -0.041 ± 0.013 leading to an uncomfortably
large M2 strength of 7 ± 5 W.u. In view of the large error, however,
the J^π = 7/2$^-$ solution can not be rejected.

The 4.85 MeV level. The angular distribution of the primary
transition at the E_p = 1015 keV resonance excludes J = 1/2 and 3/2.
Application of the RUL's to the 4.85 → 1.73 MeV transition strength
excludes J = 5/2$^-$, 7/2, 9/2. Conclusion: J^π = 5/2$^+$.

The 4.96 MeV level. The angular distributions at the E_p = 1872 keV
resonance lead to J = 3/2 (fig. 4d).

The 5.49 MeV level. Application of the RUL's on the branches to
the 3.10 and 3.71 MeV levels restricts the spin to J^π = 3/2$^-$, 5/2,
7/2$^+$. The observed mixing ratios of the 5.49 → 3.09 and 5.49 → 3.71 MeV
transitions in the E_p = 1015 keV resonance in combination with the

RUL's lead to $J^\pi = (3/2, 5/2)^+$. Conclusion: $J^\pi = 5/2^+$.

The 6.70 MeV level. The angular distributions at $E_p = 1015$ keV
yield $J = 3/2, 5/2$. The observed mixing ratio of the transition to
the 4.46 MeV level excludes $J = 3/2$. Conclusion: $J = 5/2$.

5. Summary and discussion

The extensive amount of data on resonance and bound-state decay pre-
sented in ref.[3], made it possible to select resonances suitable for the
determination of spins and lifetimes of bound states.

Measurements of angular distributions at 9 selected resonances lead to
unique spin determinations for 13 bound states. Doppler-shift measurements
resulted in lifetimes or lifetime limits for 25 bound states.

The availability of these data makes a comparison possible with cal-
culated level schemes. In the past such a comparison was not very meaning-
ful because of the scarcity of experimental data.

Only a few shell-model calculations have been performed on the level
scheme of ^{37}Cl. Excitation energies were calculated by Erné [13] in a
$1d_{3/2}^4 1f_{7/2}$ configuration space. Maripuu and Hokken [14] calculated mainly
M1 strengths of transitions between analog and anti-analog states in a
$1d_{3/2}^4 1f_{7/2}^n 2p_{3/2}^{1-n}$ space. Wildenthal et al. [12] used the complete sd shell con-
figuration space. Finally, in Hasper's calculations [15], up to three parti-
cles are promoted from the $2s_{1/2} 1d_{3/2}$ subshell to the $1f_{7/2}$ and $2p_{3/2}$ orbits.

As the level density above $E_x = 5$ MeV is high both experimentally and
theoretically, and since moreover the information about spins and parities
is scarce, no attempt is made to extend the comparison beyond this energy.

Below $E_x = 5$ MeV, the sd shell calculations [12] produce only three ex-
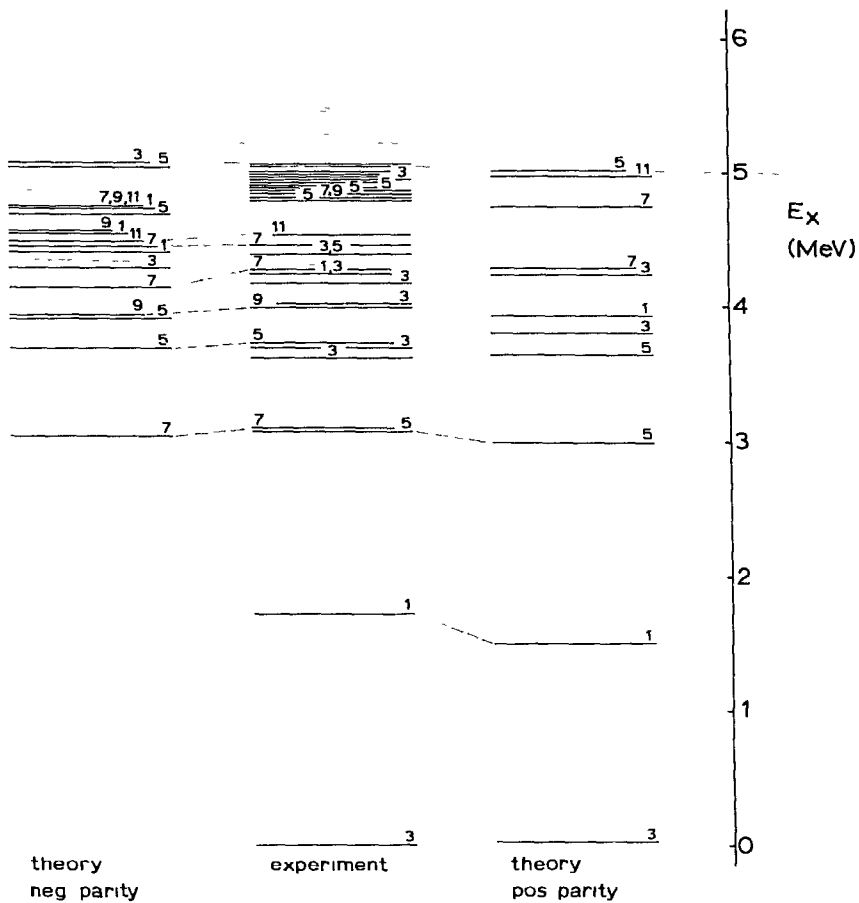
Fig. 6. Comparison of measured and calculated [15] level schemes of ^{37}Cl. The experimental data are mainly from the present work, with some additional information from ref.[1]. The levels are labelled with 2J. In the experimental level scheme the labels are placed at the right and left hand side to indicate even and odd parity, respectively. When the parity is not known, the angular momentum label is placed in the middle of the level.

cited states. They can be identified with the $E_x = 1.73$ MeV, $J^\pi = 1/2^+$, the $E_x = 3.09$ MeV, $J^\pi = 5/2^+$ and the $E_x = 3.71$ MeV, $J^\pi = 3/2^+$ levels. The calculations of Erné [13] produce many odd-parity states in this region. Quite a few can be identified with experimentally known levels, viz. those at $E_x = 3.10$, 3.74, 4.01, 4.273 and 4.55 MeV. These calculations and those of Maripuu and Hokken [14] yield many low-lying high-spin states that have not been found experimentally. The remaining even-parity states are expected to have a $1f_{7/2}^2$ character. The strong pairing of two $f_{7/2}$ particles favours this configuration. The only calculations that take this configuration into account are those of Hasper [15].

In fig. 6 the results of the latter calculations are compared with the presently available experimental data. The calculations seem to reproduce the level density rather well. The high-spin odd-parity states are reproduced very well, but several calculated even-parity states are not known experimentally and vice versa. Another discrepancy is the number of $J^\pi = 3/2^+$ levels.

Since transition strengths and lifetimes have not been calculated, however, the identification of calculated levels with experimentally known levels is not unambiguous. More detailed calculations would certainly facilitate an adequate comparison with the extensive experimental information presently available.

REFERENCES

1. P.M. Endt and C. van der Leun, Nucl. Phys. A310 (1978) 1

2. A.K. Hyder, G.I. Harris, J.J. Perrizo and F.R. Kendziorski,
   Phys. Rev. 169 (1968) 899

3. Chapter I of this thesis

4. P.M. Endt, Atomic Data and Nuclear Data Tables 23 (1979) 3

5. H.J. Rose and D.M. Brink, Revs. Mod. Phys. 39 (1967) 306

6. A.N. James, P.J. Twin and P.A. Butler, Nucl. Instr. 115
   (1974) 105

7. A.E. Blaugrund, Nucl. Phys. 88 (1966) 501

8. B.M. Paine, S.R. Kennet and D.G. Sargood, Phys. Rev. C17 (1978)
   1550

9. Appendix A of this thesis

10. P.J. Nolan, A.J. Brown, P.A. Butler, L.L. Green, A.N. James,
    J.R. Leslie, C.J. Lister, J.D. MacArthur and J.F. Sharpey-Schafer,
    J. of Phys. G2 (1976) 559.

11. P. Doll, H. Mackh, G. Mairle and G.J. Wagner, Nucl. Phys. A230
    (1974) 329

12. B.H. Wildenthal, E.C. Halbert, J.B. McGrory and T.T.S. Kuo,
    Phys. Rev. C4 (1971) 1266

13. F.C. Erné, Nucl. Phys. 84 (1966) 91

14. S. Maripuu and G.A. Hokken, Nucl. Phys. A141 (1970) 481.

15. H. Hasper, Phys. Rev. C19 (1978) 1482

APPENDIX A

SPIN J = ½ ASSIGNMENTS TO PROTON-CAPTURE RESONANCES

Abstract: Criteria are formulated for unique J = 1/2 assignments to (p,γ)
resonance levels on the basis of γ-ray angular distributions only.
For these J-assignments the angular distributions obviate the more
complicated conventional γ-γ angular correlation measurements.

In proton capture reactions on even-even target nuclei, the angular
distribution of a primary γ-ray transition between a resonance level
with spin J_r and a bound state with spin J_f, is isotropic
(i) when J_r = 1/2, or

(ii) when J_r = 3/2 and δ = -0.27 (or +3.7) for J_f = 1/2,

$$\delta = +0.26 \text{ (or } \infty \text{) for } J_f = 3/2,$$

$$\delta = +0.09 \text{ (or } +3.2 \text{) for } J_f = 5/2, \text{ or}$$

(iii) for several other J_r, δ combinations with higher J_r values, where
δ is the mixing ratio of the transition.

A measured isotropic angular distribution, although consistent with
a J_r = 1/2 assignment, thus is not sufficient for such an assignment.

In the NaI era, poor energy resolution prevented an accurate measure-
ment of the angular distribution of more than one or two primary tran-
sitions from one resonance level. For unambiguous J = 1/2 assignments
from (p,γ) reactions one therefore had to rely on more complicated
γ-γ angular correlation measurements.

With the present high-resolution Ge(Li) detectors, however, it is
feasible to measure the angular distributions of typically ten primary
(plus additional secondary) transitions from one resonance level. It
is the purpose of this letter to point out how such a large number of

isotropic angular distributions can be used for spin $J_r = 1/2$ assignments at a 99.9 % probability level.

A resonance level mainly decaying to $J_f = 1/2$ and $3/2$ levels, with possibly a weaker branch to a $J_f = 5/2$ level, is a good candidate for a $J_r = 1/2$ assignment.

Application of the recommended upper limits (RUL) [1] to selected primaries will generally exclude $J_r \geqslant 7/2$. Measured isotropy of all the primaries will in most cases exclude $J_r = 5/2$ straightforwardly. A $J_r \rightarrow J_f = 5/2 \rightarrow 1/2$ transition e.g., has an angular distribution coefficient $A_2 > +0.28$ for any quadrupole/octupole mixing ratio.

Exclusion of $J_r = 3/2$ is also possible. An isotropic angular distribution for a $J_r \rightarrow J_f = 3/2 \rightarrow 3/2$ transition implies $\delta = +0.26$ (or ∞). For an M1/E2 transition this is, although not common, definitely possible. The chance that an assumed $3/2 \rightarrow 3/2$ transition has precisely the δ-value producing an isotropic angular distribution may be estimated empirically from fig. 1.

This histogram shows the distribution of all the measured E2/M1 mixing ratios for transitions from unbound levels of odd A = 7-43 nuclei listed in ref. [1]; the values listed there as $\delta \approx 0$ have been evenly divided over the range $-0.10 < \delta < +0.10$. The arrows indicate the assumed mixing ratios discussed here. The distribution is peaked around $\delta = 0$, reflecting the fact that in light nuclei the "average" E2 width is between one and two orders of magnitude smaller than the "average" M1 width. The peaking is very sharp since transitions in self-conjugated nuclei (with even A) and transitions between bound states have been omitted from this compilation. For M2/E1 mixtures the peak will be even sharper; the δ-distribution then virtually is a delta-function (for data see also ref.[1]).

64

A conservative estimate (see fig. 1) of the fraction F of the transitions with $|\delta| > 0.20$, is $F < 20$ %; for $\delta > +0.20$ thus $F < 10$ %. An upper limit for the chance P that a 3/2 → 3/2 transition would have a mixing ratio $\delta \pm \Delta\delta$ covering the required value $\delta = +0.26$, may then be given as $P < 2 \Delta\delta$ (an overestimate based on the assumption that all transitions with $\delta > +0.20$ would fall in the bite $\delta = 0.2 - 0.3$). One measured isotropic angular distribution with a typical error of $\Delta A_2 = \pm 0.05$, for an assumed 3/2 → 3/2 transition corresponding to $\Delta\delta = \pm 0.034$, thus leads to $P < 7$ %. A similar reasoning for an assumed
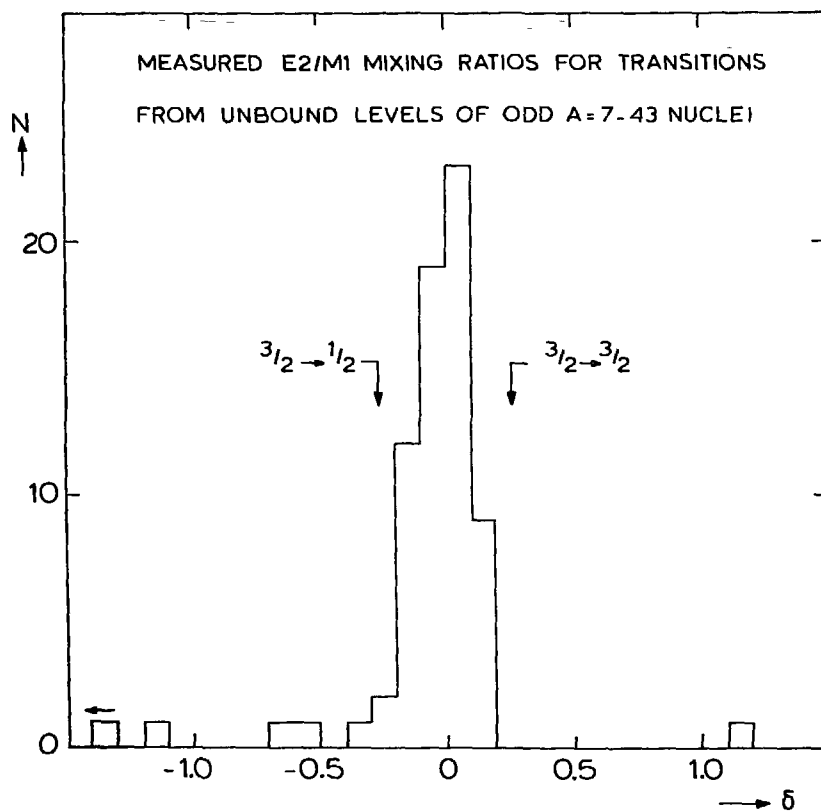
Fig. 1. Histogram of measured mixing ratios δ for E2/M1 transitions from unbound levels of odd A = 7-43 nuclei; the data are taken from ref. [1].

$J_r \to J_f = 3/2 \to 1/2$ transition gives a chance $P < 6$ %. The $J_r \to J_f = 3/2 \to 5/2$ case is less discriminating, $P < 40$ %.

Since the mixing ratios of different primary transitions are in principle not correlated, one may conclude that the chance that the primary transitions from one $J_r = 3/2$ resonance to three bound states with $J_f = 1/2$ and/or $3/2$ would accidentally produce isotropy within an uncertainty of $\Delta A_2 \leqslant 0.05$, is $P < 0.1$ %. One then may conclude to $J_r = 1/2$ at the 99.9 % confidence level. For measuring uncertainties of $\Delta A_2 \leqslant 0.08$, four in stead of three transitions would be required to reach the confidence standard generally accepted for unique spin assignments.

It might be noted that $J_r = 3/2$ can be excluded more directly if the decay proceeds to bound states with $J_f = 1/2$ and/or $3/2$, but with opposite parity. In that case at least one of the transitions would have to be an E1/M2 mixture, with the mixing ratio of $|\delta| = 0.26$ (or larger), which in most practical cases violates the RUL for M2 transitions.

The conclusion that in resonant proton capture by an even-even nucleus, the observation of a limited number of isotropic primary transitions suffices for a unique $J_r = 1/2$ assignment, may be generally and quantitatively formulated as follows. When n isotropic (and no significantly anisotropic) primaries are observed, an upper limit for the chance that the resonance has the competing spin value $J_r = 3/2$ is given by the relation $P = \prod_{k=1}^{n} a_k (\Delta A_2)_k$, where $a_k = 1.1$, 1.4 and 8 for $J_f = 1/2$, 3/2 and 5/2 (or unknown), respectively.

A few practical cases leading to $P < 0.1$ % have been mentioned above. One might add that in the extreme case that nothing would be known about the spins of the bound states, eight isotropic distributions would be

required (with $\Delta A_2 = \pm 0.05$).

This conclusion is a quantitative formulation of the qualitatively obvious difference between $J_r = 1/2$ and $J_r = 3/2$ resonances, shown in fig. 2. This figure is a histogram of the measured angular distribution coefficients of the primaries from two resonances in the $^{36}S(p,\gamma)^{37}Cl$ reaction, the $E_p = 1219$ keV, $J_r = 1/2$, and the $E_p = 699$ keV, $J_r = 3/2$ resonance [2].
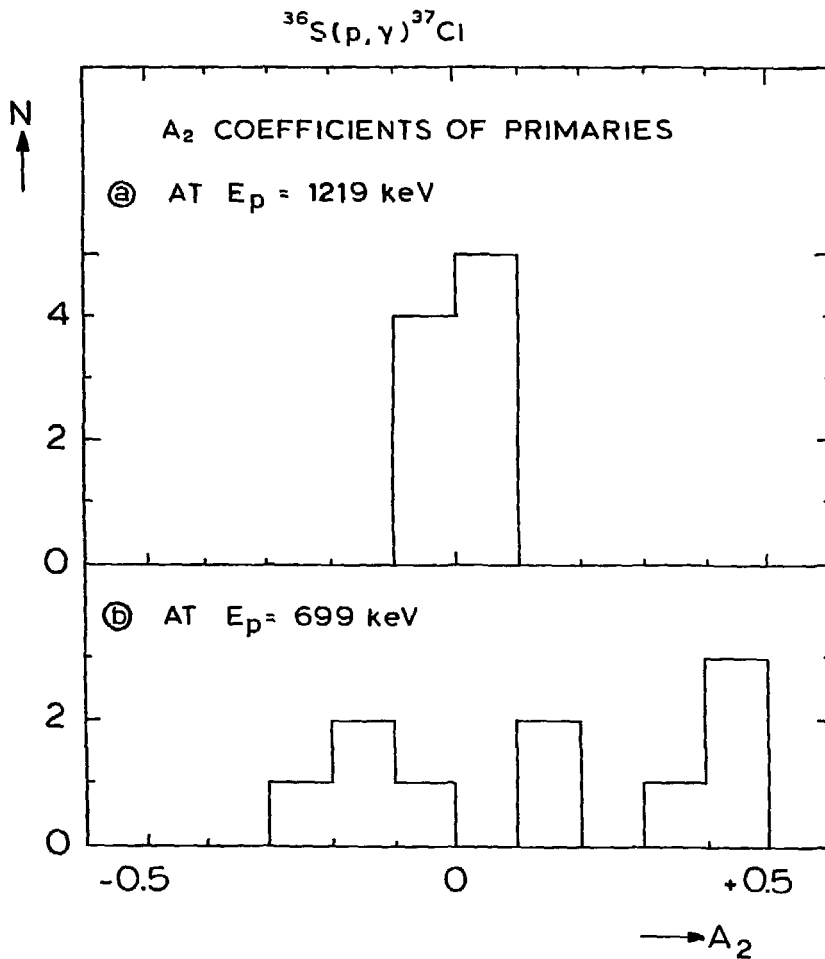

$$^{36}S(p,\gamma)^{37}Cl$$

Fig. 2. Measured angular distribution coefficients A_2 of primary γ-ray transitions at (a) the $E_p = 1219$ keV, $J_r = 1/2$ and (b) the $E_p = 699$ keV, $J_r = 3/2$ resonances in the $^{36}S(p,\gamma)^{37}Cl$ reaction; the data are from ref. [2].

Finally a few words about the three restrictions used in the above discussion.

(i) Even-even target nuclei. For target nuclei with $J \neq 0$, the method is not applicable since mixing of different orbital angular momenta adds another parameter that might produce accidental isotropy.

(ii) $J_r = 1/2$ resonances. "Anomalous" angular distributions might also be used to assign $J_r \geqslant 3/2$ or spins of bound states. In these cases, however, angular distribution measurements of primaries and secondaries will usually lead to straightforward assignments.

(iii) Resonance levels. The method can in principle also be applied for $J = 1/2$ assignments to bound states. In this case, however, the number of decay branches is usually rather low. For the most crucial rejection (of $J = 3/2$), moreover, the a_k coefficients are large, such that high-precision angular distribution measurements would be required.

In (p,γ) reaction studies with Ge(Li) detectors, simple angular distribution measurements have for some time replaced the more elaborate and time consuming γ-γ angular correlation measurements for spin assignments (see e.g. ref. [3]). This letter extends the method to unique $J_r = 1/2$ assignments. The technique is especially useful at lower proton energies, where the study of elastic proton scattering is impossible due to the small proton widths and the relatively high Rutherford cross sections. A few examples of (p,γ) resonances that can be assigned $J_r = 1/2$ on the basis of the above arguments are: the $E_p = 832$ keV $^{34}S(p,\gamma)^{35}Cl$ resonance [4], the $E_p = 924$ and 1219 keV $^{36}S(p,\gamma)^{37}Cl$ resonances [2], and the $E_p = 1107$ and 1370 keV $^{54}Fe(p,\gamma)^{55}Co$ resonances [5].

References

[1] P.M. Endt, Atomic Data and Nucl. Data Tables $\underline{23}$ (1979) 3.

[2] G.J.L. Nooren, Thesis Utrecht University (1980).

[3] J.W. Maas et al., Nucl. Phys. $\underline{A301}$ (1978) 213 and 237.

[4] M.A. Meyer et al., Nucl. Phys. $\underline{A264}$ (1976) 13.

[5] M. Adachi and C. van der Leun, to be published.

APPENDIX B

SUPPLEMENTARY INFORMATION ON THE ^{34}S(p,γ)^{35}Cl REACTION

1. Introduction

In the course of the experiments on the reaction ^{36}S(p,γ)^{37}Cl, described in this thesis, a few specific and rather detailed questions came up about the reaction ^{34}S(p,γ)^{35}Cl. These problems could be conveniently studied with the experimental set-up and the target preparation technique used in the ^{36}S(p,γ) experiments. For a description of the apparatus and the experimental methods the reader is referred to chapters I and II of this thesis. The only substantial difference is, of course, that target material enriched in ^{34}S was used. The isotopic composition was 89.8 % ^{34}S, 6.8 % ^{32}S, 2.0 % ^{33}S and 1.4 % ^{36}S.

2. Yield curve at low proton energies

The γ-ray spectrum measured at the E_p = 512 keV ^{36}S(p,γ)^{37}Cl resonance [1] contains rather strong lines from ^{35}Cl. Since the abundance of ^{34}S in the target used was at most 19 %, these background lines indicate a rather strong ^{34}S(p,γ)^{35}Cl resonance. In order to locate possible less obvious contaminant lines in other low-energy ^{36}S(p,γ)^{37}Cl resonance spectra, it was thought worthwhile to measure the ^{34}S(p,γ)^{35}Cl yield curve in the proton energy range E_p = 0.4 - 0.7 MeV, a range not covered in any of the previously

published studies on this reaction.

The yield from a 12 µg/cm^2 Ag$_2$S target was measured with a 80 cm^3 Ge(Li) detector placed at θ = 55° and a 12.5 cm × 12.5 cm ∅ NaI detector at θ = -55°. The well-known [2] resonance at E$_p$ = 716 keV was included in the measurement in order to serve as a calibration point for the resonance strength.

The yield in the E$_\gamma$ = 4 - 5 MeV channel, measured with the NaI detector is shown in fig. 1. Contaminant peaks are seen due to well-known resonances in the reactions ^{15}N(p,αγ)^{12}C, ^{19}F(p,αγ)^{16}O, ^{13}C(p,γ)^{14}N and ^{36}S(p,γ)^{37}Cl. Since the latter reaction is not a common contaminant, the γ-ray spectrum was measured to determine its origin. Apart from the contaminant and calibration resonances the curve shows only one resonance due to the ^{34}S(p,γ)^{35}Cl reaction. The value E$_p$ = 698.7 ± 0.2 keV for the ^{36}S(p,γ)^{37}Cl resonance served as an energy calibration point and yields E$_p$ = 510.6 ± 0.6 keV for the new ^{34}S(p,γ) resonance and E$_p$ = 714.8 ± 0.5 keV for the resonance for which Meyer et al.[2] find E$_p$ = 716.0 ± 1.0 keV.

The 511 keV resonance decays to ^{35}Cl levels at E$_x$ = 0, 1.22, 2.69, 4.06, 4.08 and 5.01 MeV, with branchings of 33, 24, 14, 5, 6 and 8 %, respectively (10 % of the decay is unknown). This
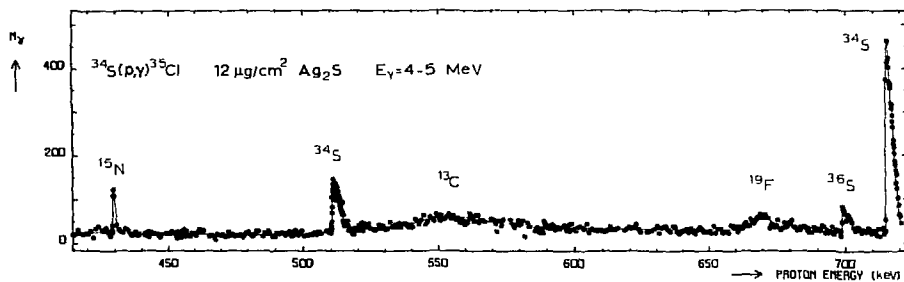

Fig. 1. Yield curve of the reaction ^{34}S(p,γ)^{35}Cl over the proton energy range E$_p$ = 0.4 - 0.7 MeV. The 12 µg/cm^2 Ag$_2$S target was prepared from sulphur enriched to 90 % ^{34}S.

exclusive decay to J = 1/2 and 3/2 levels indicates a low reso-
nance spin, as could be expected.

The resonance strength is $(2J + 1)\Gamma_p\Gamma_\gamma/\Gamma = 0.05 \pm 0.02$ eV.
Any other resonances in the range $E_p = 0.4 - 0.7$ MeV have a strength
of at most 0.02 eV.

3. The largest observed M2 strength

A recent review [3] of γ-ray transition strengths recommends
an upper limit (RUL) for M2 strengths of 3 W.u. The RUL's are
widely used, also in the present thesis, for spin rejections for
which otherwise (e.g. in the analysis of angular distribution
measurements) a 99.9 % confidence limit is standardly used. It
therefore is highly disturbing that an M2 strength has been
measured of 3.1 ± 1.0 W.u. The relatively large error in this
measured M2 strength is given [3] as an excuse for not increasing
the RUL for M2, but some nesitance about the correctness of the
published value may also have influenced this decision.

The M2 transition of 3.1 W.u. mentioned above, occurs in the
ground-state decay of the E_p = 1468 keV $^{34}S(p,\gamma)^{35}Cl$ resonance.
The resonance spin has been reported as $J_r = 3/2$ on the basis of
γ-ray angular distribution measurements [2] and as $J_r^\pi = (1/2,3/2)^-$
with some preference for $J_r^\pi = 1/2^-$ on the basis of $^{34}S(p,p_0)^{34}S$
work [4]. The combination of these two pieces of information leads
to the assignment $J_r^\pi = 3/2^-$ given by Endt and Van der Leun [5].
The reported mixing ratio of the $3/2^- \rightarrow 3/2^+$, r → 0 transition,
$\delta \approx 0.33 \pm 0.02$, combined with the (p,γ) resonance strength and
branching ratio, then leads to the large M2 strength.

72

Two steps in the above deduction of the resonance spin have been checked in the present experiment.

First the γ-ray yield curve over the E_p = 1468 keV resonance was measured with the high-resolution Utrecht 3 MV Van de Graaff accelerator. A possible doublet character would invalidate the identification of the (p,γ) and (p,p_0) resonances which is an essential step in the $J^\pi = 3/2^-$ assignment. The E_p = 1468 keV (p,γ) resonance peak turns out to have a width that is not measurably larger than that of neighbouring resonances. Comparison of the yield curves for several different channel settings, each corresponding to specific transitions, does not reveal any measurable energy shifts. Summarizing, there is no evidence for a doublet character of this resonance.

Secondly, the J_r = 3/2 assignment based on previous (p,γ) work was checked. Gamma-ray angular distributions were measured in which the isotropic 1.22 → 0 MeV, J = 1/2 → 3/2 transition was used as a monitor, thus circumventing any eccentricity problems. The deduced angular distribution coefficients A_2 are presented in table 1 and compared with the values found in ref.[2]. Application of the method discussed in Appendix A to the five primary transitions, leads to a unique J_r = 1/2 assignment, in contradiction to previous (p,γ) work [2], but in line with the $J_r^\pi = (1/2)^-$ assignment from the (p,p_0) experiments [4]. Conclusion: $J_r^\pi = 1/2^-$.

In ref.[2] a J = 1/2 assignment was excluded essentially on the basis of the measured A_2 = -0.06 ± 0.02 coefficient for the r → 0 transition. The present work suggests that Meyer et al.[2] underestimated the experimental errors. This suggestion is supported by the observation that in ref.[2] the χ^2 values given for accepted J-values are significantly larger than the expected average value χ^2 = 1.

The mixing ratio for the $1/2^- → 3/2^+$, r → 0 transition could not

be determined in the present experiment, but the J_r = 1/2 assignment invalidates the previously reported value of δ = +0.33 and thus the M2 admixture of 3.1 W.u. Similarly the 0.34 ± 0.16 W.u. M2 admixture in the r → 1.22 MeV transition should be eliminated from the list of measured M2 transition strengths.

4. Capture and scattering resonances

The information on resonance levels deduced from the reactions $^{34}S(p,\gamma)^{35}Cl$ [refs.[2,6]] and $^{34}S(p,p)^{34}S$ [ref.[4]] is generally in excellent agreement. One exception, the E_p = 1468 keV resonance, has been discussed above. A second problem is the E_p = 2531 keV resonance.

Table 1

Angular distribution coefficients of γ-rays
from the E_p = 1468 keV $^{34}S(p,\gamma)^{35}Cl$ resonance

$E_{xi} \rightarrow E_{xf}$ (MeV)	A_2	
	Present work	Ref.[2]
r → 0	0.006 ± 0.014	-0.06 ± 0.02 [a]
→ 1.22	-0.03 ± 0.03	-0.02 ± 0.06 [b]
→ 5.01	-0.07 ± 0.04	
→ 5.40	0.04 ± 0.05	
→ 5.65	0.03 ± 0.08	

[a] And A_4 = -0.03 ± 0.02 instead of the expected $A_4 \cong 0$ for J_r = 3/2.

[b] And A_4 = -0.14 ± 0.07 instead of $A_4 \cong 0$.

In the elastic scattering experiment [4] a resonance has been found at E_p = 2527 ± 3 keV with $J_r^\pi = 1/2^+$, whereas a capture resonance has been reported at E_p = 2531.4 ± 0.5 keV that decays strongly (33 %) to the E_x = 2.65 MeV, $J^\pi = 7/2^+$ level of ^{35}Cl, implying $J_r \geqslant 3/2$. This apparent discrepancy prompted a detailed check of the (p,γ) data.

The yield curve for capture γ-rays was measured with a fixed accelerator voltage by applying a triangle shaped voltage of about 7 kV amplitude to the target. The raw data were labelled with the digitized voltage and written on magnetic tape. In the off-line analysis of these data, yield curves were constructed for the different decay modes and γ-ray spectra for different E_p values over the yield curve. Neither the γ-ray spectra nor the separate yield curves gave any evidence for a doublet. The decay scheme deduced from the γ-ray spectra mentioned above, confirms the findings of Sparks [6]. We conclude that two different resonances are excited in the ^{34}S(p,γ) and ^{34}S(p,p) resonances at E_p = 2531 keV.

References
_____

1. This thesis, chapter I
2. M.A. Meyer et al., Nucl. Phys. A264 (1976) 13
3. P.M. Endt, Atomic Data and Nucl. Data Tables 23 (1979) 3
4. D.A. Outlaw, G.E. Mitchell and E.G. Bilpuch, Nucl. Phys. A284 (1977) 1
5. P.M. Endt and C. van der Leun, Nucl. Phys. A310 (1978) 1
6. R.J. Sparks, Nucl. Phys. A265 (1976) 416

SAMENVATTING

Onze kennis van aangeslagen toestanden van de kern ^{37}Cl is tot nu toe uiterst beperkt. Het overzicht van Endt en Van der Leun vermeldt van deze kern slechts elf toestanden met bekende spin. Ook over levensduren, vervalswijzen en excitatie-energieën is weinig bekend. Van de lichte kernen is ^{37}Cl een van de minst onderzochte en slechtst bekende stabiele kernen.

Dit gebrek aan kennis wordt veroorzaakt door het probleem van het aanslaan van deze kern. Behalve door protonvanst in ^{36}S is deze kern bestudeerd met inelastische protonverstrooiing, met de reactie ^{34}S(α,pγ)^{37}Cl, die een kleine werkzame doorsnede heeft, met de oppakreactie ^{38}Ar(d,τ)^{37}Cl, die tot nu toe slechts is uitgevoerd met slecht scheidend vermogen, en via nog enige andere reacties, alle met een laag rendement voor de productie van spectroskopische gegevens. Het betaverval van ^{37}S heeft ook nog enige informatie opgeleverd.

De protonvangstreactie is zeer doelmatig voor de spectroskopie vanwege haar niet-selectief karakter. Door de aard van het proces worden echter alleen toestanden met een laag impulsmoment aangeslagen. De vergeleken met de andere bovengenoemde reacties kleine werkzame doorsnede van deze react*? wordt grotendeels gecompenseerd door de grote protonbundelstroor die bij de Utrechtse 3 MV Van de Graaffgenerator beschikbaar is. Vergeleken met reacties waarbij het gebruik van coïncidentietechnieken noodzakelijk is, zijn de bruikbare gammastralingsfluxen van dezelfde grootte-orde.

Voor de bestudering van ^{37}Cl kan deze reactie niet zonder meer gebruikt worden vanwege het lage percentage waarmee ^{36}S in de natuur voorkomt. De samenstelling van natuurlijk zwavel is: 95% ^{32}S, 0,75% ^{33}S, 4,2% ^{34}S en 0,017% ^{36}S. Gedurende lange tijd was slechts

76

matig verrijkt (3,5%) materiaal beschikbaar, waarin het gehalte aan
^{36}S nog lager was dan het gehalte ^{34}S. Het onderscheiden van de reacties
op de twee isotopen gaf dan ook problemen, terwijl tevens de gevoelig-
heid tamelijk klein was. Met een isotopenseparator kunnen wel trefplaat-
jes worden geïmplanteerd met zuiver ^{36}S, maar de proton-energiespreiding
die ontstaat in het dragermateriaal reduceert dan het scheidend ver-
mogen.

Het huidige, hoogverrijkte en zeer kostbare materiaal kon dankzij
een speciale techniek gebruikt worden om goede trefplaatjes te maken
met minieme hoeveelheden ^{36}S. Het gebruikte zilversulfide vormt een
dunne, stabiele, uniforme laag, die een geringe energiespreiding ver-
oorzaakt. Dankzij een speciaal ontworpen trefplaathouder met sterk
verbeterde koeling kan ook daadwerkelijk gebruik gemaakt worden van
de beschikbare grote bundelstromen, zonder dat de slijtage van de
trefplaatjes ontoelaatbaar groot wordt.

De opbrengst van vangstreacties vertoont sterke pieken, resonanties,
bij bepaalde protonenergieën. Deze resonanties zijn hoog aangeslagen
toestanden die deels door uitzending van gammastraling vervallen.
Dit verval verloopt meestal indirect, via andere aangeslagen toestan-
den, de gebonden niveaus. Eigenschappen van deze gebonden toestanden
kunnen worden afgeleid uit metingen van de gammastraling van de reso-
nanties. Een deel van het eerste hoofdstuk is gewijd aan resonanties.
Ze worden gevonden door de reactieopbrengst te meten als functie van
de versnelspanning en dus de protonenergie. Van 187 resonanties werd
de energie, de sterkte en in enkele gevallen ook de breedte bepaald,
van 75 tevens het verval. Bij het verval van de resonanties zijn we
met name geïnteresseerd in de mate waarin dit verval geschiedt via
nog slecht bekende of geheel onbekende toestanden. Er werden op deze
manier 28 nieuwe toestanden gevonden en het verval van 54 toestanden

kon bestudeerd worden. Met behulp van speciale experimenten werd de
aanslagenergie van gebonden toestanden bepaald met een nauwkeurigheid
beter dan 1 op 10000. Ook de reactie-energie, belangrijk voor de
systematiek van atoommassa's, kon met een dergelijke precisie bepaald
worden.

Deze gegevens worden gebruikt bij metingen voor de bepaling van
spins en levensduren, het onderwerp van het tweede hoofdstuk. Voor
het bepalen van levensduren is het Dopplereffect gebruikt. Door de
grote snelheid van het inkomend proton zal de gevormde ^{37}Cl kern
een snelheid krijgen van ca. 0,1 % van de lichtsnelheid, waardoor de
waargenomen gammastraling Dopplerverschuiving zal vertonen. Uit
metingen van de grootte van deze verschuiving kunnen, indien het
afremproces bekend is, levensduren van aangeslagen toestanden wor-
den berekend. Spins worden bepaald uit metingen van de hoekafhanke-
lijkheid van de intensiteit van de gammastraling. Door de eenvoud
van het vangstproces in even-even trefplaatkernen zoals ^{36}S, leidt
dit op vrij simpele wijze tot het bepalen van spins. De aanwezig-
heid van een isotrope, niet hoekafhankelijke vervalslijn in de meeste
resonanties vereenvoudigt de opstelling en leidt tot een verkleining
van systematische fouten. Dankzij dit alles en uitgaande van de ge-
gevens verzameld in het eerste hoofdstuk, konden tot nu toe 21 spins
en 17 levensduren bepaald worden.

Vergelijking van deze gegevens met enkele eerder gepubliceerde
theoretische berekeningen verschaft inzicht omtrent de structuur
van een aantal niveaus van ^{37}Cl. De vergelijking zou duidelijk aan-
trekkelijker worden wanneer meer gedetailleerde berekeningen aan
deze kern kunnen worden uitgevoerd. Indien deze ook overgangswaar-
schijnlijkheden opleveren kunnen de gemeten levensduren, vertak-
kings- en mengverhoudingen ook in de vergelijking worden betrokken.

78

In appendix A wordt aandacht gegeven aan de spin J = 1/2 toe-
kenningen aan resonantieniveaus. Op empirische gronden wordt een
regel voorgesteld, die aangeeft onder welke voorwaarden een een-
duidige spin J = 1/2 toekenning gerechtvaardigd is.

Appendix B bespreekt enkele detailproblemen uit de reactie
$^{34}S(p,\gamma)^{35}Cl$, die voor het merendeel gerelateerd zijn aan de in
dit proefschrift beschreven $^{36}S(p,\gamma)^{37}Cl$ metingen. Zo is aangetoond
dat de enige gepubliceerde M2 sterkte die de aanbevolen bovengrens
(RUL) overschrijdt, en die zodoende invloed zou kunnen hebben op
de in ons werk verkregen resultaten, op een meetfout berust.

79

CURRICULUM VITAE

Na zijn gymnasium-opleiding begon de schrijver in 1968 zijn studie in de technische natuurkunde aan de T.H. Delft. Het kandidaats- en afstudeerwerk werd verricht in de vakgroep experimentele kernfysica van prof. A.H. Wapstra. Na het behalen van het ingenieursdiploma in 1974 vervulde de schrijver zijn militaire dienstplicht. Deze bracht hij grotendeels door als gedetacheerde op het Physisch Laboratorium van de Rijksverdedigingsorganisatie. Hij onderzocht daar de mogelijkheden om eigenschappen van atmosferische aerosolen te bepalen met behulp van een laser-radar. In 1976 trad hij, als promovendus bij de vakgroep kernfysica, in dienst van de Stichting FOM. Het onderzoek dat in dit proefschrift beschreven wordt, vond grotendeels plaats in de periode van begin 1978 tot heden. Naast zijn onderzoek assisteerde hij bij het voorkandidaats onderwijs aan studenten in de medicijnen en de biologie.